Research

Transthyretin-Binding Activity of Complex Mixtures Representing the Composition of Thyroid-Hormone Disrupting Contaminants in House Dust and Human Serum

Timo Hamers,[1] Andreas Kortenkamp,[2] Martin Scholze,[2] Douwe Molenaar,[3] Peter H. Cenijn,[1] and Jana M. Weiss[4]

[1]Department of Environment and Health, Vrije Universiteit Amsterdam, Amsterdam, Netherlands
[2]Institute of Environment, Health and Societies, Brunel University, London, UK
[3]Department of Systems Bioinformatics, Vrije Universiteit Amsterdam, Amsterdam, Netherlands
[4]Department of Environmental Science and Analytical Chemistry, Stockholm University, Stockholm, Sweden

BACKGROUND: House dust contains many organic contaminants that can compete with the thyroid hormone (TH) thyroxine (T_4) for binding to transthyretin (TTR). How these contaminants work together at levels found in humans and how displacement from TTR *in vitro* relates to *in vivo* T_4-TTR binding is unknown.

OBJECTIVES: Our aims were to determine the TTR-binding potency for contaminant mixtures as found in house dust, maternal serum, and infant serum; to study whether the TTR-binding potency of the mixtures follows the principle of concentration addition; and to extrapolate the *in vitro* TTR-binding potency to *in vivo* inhibition levels of T_4-TTR binding in maternal and infant serum.

METHODS: Twenty-five contaminants were tested for their *in vitro* capacity to compete for TTR-binding with a fluorescent FITC-T_4 probe. Three mixtures were reconstituted proportionally to median concentrations for these chemicals in house dust, maternal serum, or infant serum from Nordic countries. Measured concentration–response curves were compared with concentration–response curves predicted by concentration addition. For each reconstituted serum mixture, its inhibitor–TTR dissociation constant (K_i) was used to estimate inhibition levels of T_4-TTR binding in human blood.

RESULTS: The TTR-binding potency of the mixtures was well predicted by concentration addition. The $\sim 20\%$ inhibition in FITC-T_4 binding observed for the mixtures reflecting median concentrations in maternal and infant serum was extrapolated to 1.3% inhibition of T_4-TTR binding in maternal and 1.5% in infant blood. For nontested mixtures reflecting high-end serum concentrations, these estimates were 6.2% and 4.9%, respectively.

DISCUSSION: The relatively low estimated inhibition levels at median exposure levels may explain why no relationship between exposure to TTR-binding compounds and circulating T_4 levels in humans has been reported, so far. We hypothesize, however, that 1.3% inhibition of T_4-TTR binding may ultimately be decisive for reaching a status of maternal hypothyroidism or hypothyroxinemia associated with impaired neurodevelopment in children. https://doi.org/10.1289/EHP5911

Introduction

Over the past decade, awareness has increased that house dust is a matrix containing complex mixtures of contaminants. Most of these contaminants originate from the use and wear of household products and building materials; indoor activities such as cooking, smoking, and incineration of (household) products; and the intrusion of outdoor material (Mercier et al. 2011). In an inventory of contaminants reported in house dust, Zhang et al. (2015) found 485 organic compounds, including alkyl-phenols and their ethoxylates, phthalates, parabens, musks, perfluoroalkyl substances (PFASs), brominated flame retardants (BFRs) including polybrominated diphenyl ethers (PBDEs), organophosphorous flame retardants (OPFRs), polychlorinated biphenyls (PCBs), polyhalogenated dibenzo-*p*-dioxins and dibenzofurans (PXDD/Fs) polycyclic aromatic hydrocarbons, chlorinated benzenes, polychlorinated naphthalenes, organo-siloxanes, volatile organic compounds, ultraviolet (UV)-filter related chemicals, biocides, and pesticides.

Indoor exposure to house dust contaminants may occur through inhalation, dermal contact, and ingestion. The importance of the latter route has been mainly demonstrated for PBDEs. The contribution of house dust ingestion to the total PBDE intake in adults appears to be in the same order of magnitude as the contribution of dietary exposure, although estimates differ considerably between countries (Besis and Samara 2012; SK Kim et al. 2016). More importantly, these studies concluded that house dust ingestion is the major route of PBDE exposure for toddlers, who have lower dietary intake but higher house dust ingestion than adults due to their relatively long residence time on the floor and frequent hand-to-mouth contact. Given the high number of contaminants demonstrated in house dust, it is to be expected that house dust ingestion especially by toddlers may be an underestimated route of human exposure to compounds other than PBDEs (De Boer et al. 2016).

Many house dust contaminants are known to be thyroid-hormone (TH) disrupting compounds (Zhang et al. 2015), such as phenols, phthalates, parabens, PFASs, PBDEs, OPFRs, PCBs, PXDD/Fs, UV filters, and biocides. Some of these chemicals have been reported to antagonize thyroid receptor (TR) activity (Klopčič et al. 2016; Kollitz et al. 2018; Zhang et al. 2016). Others have been shown to activate the nuclear receptors pregnane X receptor (PXR), constitutive androstane receptor (CAR) (Kretschmer and Baldwin 2005), or arylhydrocarbon receptor (AhR) (Denison and Nagy 2003), thereby inducing the expression and activity of uridine diphosphate glucuronosyltransferase (UGT) isoforms 1A1 and 1A6 (Shelby and Klaassen 2006), which are responsible for an increased glucuronidation (Roos et al. 2011; Vansell and Klaassen 2002) and subsequent hepatic clearance (Liu et al. 1995) of TH. Still others have been shown to inhibit the sodium iodide symporter (NIS) (Hallinger et al. 2017; Wang et al. 2018) or thyroid peroxidase (TPO) (Paul et al. 2014), which are involved in TH synthesis. In the present study, we focus on the TH distributor protein transthyretin (TTR) as a target for TH disrupting compounds. Together with TH binding globulin (TBG) and albumin (ALB), TTR is one of the three plasma carrying proteins transporting TH from the thyroid gland to the peripheral (target) tissues. Although triiodothyronine (T_3) is the

actual active form of TH, these distributor proteins have a higher affinity for its precursor thyroxine (T_4) (Salvatore et al. 2016). Many xenobiotic substances, including house dust contaminants, are capable of competing with T_4 for binding to TTR (Weiss et al. 2015; Zhang et al. 2016). As a consequence, diminished amounts of TTR-bound T_4 is stored in the blood plasma and correspondingly larger amounts of free T_4 are available for biliary elimination via hepatic uptake and conjugation, causing a decrease in free and total plasma T_4 levels, as observed in rodents exposed to TTR-binding compounds (Darnerud et al. 1996; Hallgren and Darnerud 2002). T_4 deficiency has been implicated in neurodevelopmental effects on cognition in rodents (Taheri et al. 2018) and humans (Korevaar et al. 2016). Moreover, TTR-binding PCB metabolites were shown to accumulate in blood plasma of laboratory rats (Bergman et al. 1994), free-ranging polar bears (Gutleb et al. 2010), and human populations (Athanasiadou et al. 2008; Park et al. 2008) and may ultimately be transported across the placenta where they have been demonstrated in fetal rat brain (Meerts et al. 2002) and in human cord blood (Park et al. 2008), most likely due to TTR-mediated transport. It cannot be excluded that this transport route also holds for other persistent TTR-binding compounds.

To our knowledge, the contribution of multiple chemicals present in house dust to displacing T_4 from TTR has not been investigated. Accordingly, the goal of the present study was *a*) to determine the TTR-binding potency of complex mixtures of house dust contaminants representing the composition as found in human blood and in house dust; *b*) to study whether the TTR-binding potency of the complex mixtures could be predicted by weighing the concentration of each individual constituent of the mixture for its TTR-binding potency, according the principle of concentration addition; and *c*) to extrapolate the TTR-binding capacity of the mixtures in an *in vitro* binding assay to *in vivo* inhibition levels of T_4-TTR binding in human maternal and infant blood.

Altogether, a set of 25 compounds was selected and tested individually for their capacity to bind to TTR in a competitive binding assay. In addition, three different mixtures were reconstituted reflecting the composition of the selected chemicals based on median concentrations reported in house dust, maternal serum, or in serum from cord blood/infants (hereafter referred to as infants). These mixtures were also tested in the TTR-binding assay to confirm that the principle of concentration addition holds for such complex mixtures. In addition, the mixture experiments allowed us to determine a margin of exposure between the actual median mixture concentration in serum from infants and mothers on the one hand and the observed effect levels in the *in vitro* TTR-binding assay on the other hand. More importantly, the *in vitro* TTR-binding potencies of the mixtures were extrapolated to actual *in vivo* TTR-binding potencies in maternal or infant blood, taking into account the binding of TH to the other two plasma distributor proteins, TBG and ALB. As such, the concentrations in human plasma of TTR-binding inhibitors were calculated into predicted effect levels in humans.

Material and Methods

Test Compound Selection

Test compounds were selected based on three different criteria:
1. The compounds should be present in house dust, or—in the case of metabolites—their parent compound should be present in house dust. To meet this criterion, all selected compounds or their parent compounds should be listed in the inventory of 485 house dust contaminants made by Zhang et al. (2015).
2. The TTR-binding capacity of the compounds or their metabolites should have been experimentally confirmed. Weiss

et al. (2015) compiled a database of 144 compounds capable of competing with TH for TTR-binding. As was to be expected based on structural similarity with TH, many TTR-binding compounds were halogenated phenols (including metabolites of PBDEs, PCBs, and PXDD/Fs), but PFASs and other (mainly halogenated) compounds were also identified as TTR-binders.
3. Their concentration in dust, maternal serum, or cord blood/infant serum should be known. For compounds meeting the first two criteria, data on median levels in dust, in maternal serum, and in cord blood/infant serum were collected in 2016 from Swedish studies or alternatively European, preferably Nordic, studies reported in the open literature. The selection of Swedish studies was based on the fact that the present study was performed within a Swedish research project called MiSSE (Mixture aSSessment of Endocrine disrupting compounds with emphasis on the TH system). MiSSE has determined concentrations for many house dust contaminants in Swedish household dust. Many of these concentrations were used in the present study. To obtain geographic correspondence between chemical profiles in house dust and human serum, the present study gave preference to the utilization of Swedish, or else Nordic, serum levels.

The set of 25 selected test chemicals consisted of the following compounds: perfluorohexanoic acid (PFHxA), perfluoroheptanoic acid (PFHpA), perfluorooctanoic acid (PFOA), perfluorononanoic acid (PFNA), perfluorodecanoic acid (PFDA), perfluoroundecanoic acid (PFUnDA), perfluorobutane sulfonic acid (PFBS), perfluorohexane sulfonic acid (PFHxS), perfluorooctane sulfonic acid (PFOS), perfluorooctane sulfonamide (FOSA), propyl 4-hydroxybenzoate (propylparaben), 4-nonylphenol, pentachlorophenol, 5-chloro-2-(2,4-dichlorophenoxy)phenol (triclosan), tetrabromo-bisphenol-A (TBBPA), 2,4,6-tribromophenol (2,4,6-TBP), 2,2′,4,4′-tetrabromodiphenyl ether (BDE-47) and its metabolites 5-OH-2,2′,4,4′-tetrabromodiphenyl ether (5-OH-BDE-47) and 6-OH-2,2′,4,4′-tetrabromodiphenyl ether (6-OH-BDE-47), 2,2′,4,4′,5-pentabromodiphenyl ether (BDE-99) and its metabolite 6′-OH-2,2′,4,4′,5-pentabromodiphenyl ether (6′-OH-BDE-99), 2,3′,4,4′,5-pentachlorobiphenyl (CB-118) and its metabolite 4-OH-2,3,3′,4′,5-pentachlorobiphenyl (4-OH-CB-107), and 2,2′,4,4′,5,5′-hexachlorobiphenyl (CB-153) and 4-OH-2,2′,3,4′,5,5′,6-heptachlorobiphenyl (4-OH-CB-187). All test compounds, together with their supplier, Chemical Abstract Service number, and median or high-end (i.e., maximum or 95th percentile) concentrations reported in house dust, maternal and infant blood from Nordic countries are listed in Excel Tables S1 and S2. These Tables further specify whether infant concentrations refer to concentrations in cord blood or in children and provide references to the original publications.

Test Solutions and Mixture Reconstitution

For most of the selected compounds, stock solutions (10 or 100 mM) and subsequent dilution series were prepared in tetrahydrofuran (THF). To test the individual compounds in the bioassay, stock solutions in dimethyl sulfoxide (DMSO) were prepared by the addition of 200 μL of DMSO to 200 μL of the THF solutions followed by THF evaporation under a gentle nitrogen flow. To reconstitute a mixture, for each individual compound a precalculated volume corresponding to its ultimate molar fraction in the mixtures was taken from the THF stock or its respective dilution. After pooling these THF volumes for all compounds, 500 μL of DMSO was added, followed by THF evaporation. Perfluoroalkyl sulfonic acids (PFSAs) were not dissolved in THF, given the polymerization reaction of THF with highly acidic short-chained PFSAs (Pruckmayr and Wu 1978), also observed for PFBSs in this study. Instead, PFSAs were

directly dissolved and further diluted in DMSO. During mixture reconstitution, PFSAs (in DMSO) were added last. The ultimate 500-µL volume of DMSO added to the mixture was adjusted accordingly. All DMSO stocks of individual compounds and mixtures were further diluted in DMSO for dose–response testing in the bioassay. During mixture reconstitution, all pipetting steps were weighed, allowing the exact determination of the concentrations in the test mixtures. These actual concentrations (see Table S1) based on weights—and not the originally targeted nominal concentrations—were further used in data analyses. Differences between the actual and the targeted molar contributions to the mixture were at maximum 2.2% but were <1% in 95% of the cases.

Dust Extraction

To determine the contribution of the compounds tested in the present study to the overall TTR-binding potency in house dust, the extract of a well-characterized dust sample, for which many analytical data were available, was tested in the TTR-binding assay. For this purpose, the Standard Reference Material® 2585 (SRM2585) dust sample was purchased from the National Institute of Standards and Technology (NIST) and extracted according to Van den Eede et al. (2012). Briefly, 70 mg of dust was extracted three times with an isohexane:acetone 3:1 (vol/vol) mixture by vortexing followed by ultrasonication. After each consecutive extraction, dust was pelleted by centrifugation and the supernatant was pooled. The solvent was evaporated under a gentle nitrogen flow and the extracts were transferred to 200 µL of DMSO.

TTR-Binding Assay

The TTR-binding potency of the individual compounds, the reconstituted mixtures, and the SRM2585 extract was tested in a competitive binding assay making use of a fluorescent conjugate of T_4 and fluorescein 5-isothiocyanate (FITC). The method originally developed by Ren and Guo (2012) was previously transformed into a 96-well plate format (Ouyang et al. 2017) and further modified and optimized (Leusch et al. 2018) in our laboratory. The FITC-T_4 conjugate shows high fluorescence when its T_4 group is bound to TTR. In the presence of competitive TTR-binding compounds, a decrease in bound FITC-T_4 can be quantified as a decrease in fluorescence, which is due to the intramolecular quenching of the fluorescein group by the free T_4 group.

The FITC-T_4 conjugate was synthesized as described by Ren and Guo (2012). Briefly, 0.5 mL of 20-mg/mL FITC was reacted with 1.0 mL of 10-mg/mL T_4 (both dissolved in a mixture of 9 mL pyridine, 1.5 mL ultrapure water, and 0.1 mL triethylamine) for 1 h at 37°C. The FITC-T_4 conjugate was consecutively precipitated, centrifuged, washed, centrifuged, redissolved, and purified on a Sephadex® LH20 column. After elution with ultrapure water, the FITC-T_4 concentration was determined photospectrometrically using a molar extinction coefficient of $\varepsilon = 7.8 \times 10^4 \ M^{-1}cm^{-1}$ (Ren and Guo 2012). The FITC-T_4 solution was aliquoted and stored at −80°C.

All TTR-binding experiments were performed in black 96-well polystyrene nonbinding plates (Greiner Bio-One). Given the minimized adsorption to the wall of these well plates, nominal concentrations of FITC-T_4, TTR, and test compounds could be used in the data analysis as total concentrations of ligand, binding protein, and inhibitor, respectively. All incubations were performed for 2 h at 4°C (on ice) in a final volume of 200 µL Tris-HCl buffer (pH 8.0). Fluorescence [expressed as arbitrary fluorescence units (AFUs)] was measured at $\lambda_{ex} = 490$ nm and $\lambda_{em} = 518$ nm.

The dissociation constant K_d of the FITC-T_4-TTR complex was determined in a saturation experiment with a fixed concentration of TTR (30 nM), various concentrations of FITC-T_4 (ranging from 0 to 1,000 nM), and no inhibitor. Competitive TTR-binding assays were performed by incubating human TTR (30 nM) with 110 nM of FITC-T_4 in the presence of test compounds, reference compound T_4, or carrier solvent control (1% DMSO). For each incubation with TTR, a parallel incubation was performed without TTR to correct for background fluorescence of the unbound FITC-T_4. In the competitive binding experiments, these control incubations were also used to check for possible quenching of FITC-T_4 fluorescence by the test compounds and for autofluorescence of the test compounds themselves, neither of which was observed. Altogether, on each 96-well plate three different compounds or mixtures were tested in duplicate with and without TTR in a concentration series of seven concentrations and a solvent control. Each compound, each reconstituted mixture, and the SRM2585 dust extract was tested in two independent experiments, except for the reference compound T_4, which was tested in 21 experiments altogether. All experiments were performed within a period of 4 weeks.

Background Correction

All fluorescence measurements were corrected for protein-independent fluorescence by subtracting the measured fluorescence in the absence of protein from the measured fluorescence in the presence of protein. The obtained corrected fluorescence (F_c) is directly proportional to the concentration of the protein–ligand complex [PL] as demonstrated in "S1.2 Corrected fluorescence is proportional to [PL]" in the Supplemental Material, based on the basic principles of protein–ligand binding in the presence of a competitive inhibitor described in "S1.1 Basic principles of protein-ligand binding in the presence of a competitive inhibitor."

K_d Estimation

F_c values of the saturation experiment, expressed in AFUs, could consequently be described as a function of the total ligand concentration (L_T)

$$F_c = a \times [PL]$$
$$= a \times \frac{(K_d + [P_T] + [L_T]) - \sqrt{(K_d + [P_T] + [L_T])^2 - 4 \times [P_T] \times [L_T]}}{2},$$
(1)

with a being the ratio between F_c and [PL], [P_T] is the total protein concentration (i.e., [TTR] = 30 nM), and [L_T] is the total ligand concentration ranging from 0 to 1,000 nM FITC-T4 in the saturation experiment. Parameters a and K_d were estimated by nonlinear regression between [L_T] and F_c. The theory behind Equation 1 and its derivation have been described in detail in "S1.3 K_d assessment" in the Supplemental Material, based on Neubig (2011).

Concentration–Response Analysis

For the competitive binding experiments, the corrected fluorescence measurements were used to fit concentration–response curves and derive the concentration causing 20% and 50% inhibition of TTR-binding by FITC-T_4 (IC_{20} and IC_{50}, respectively). Similarly, concentration–response curves with corresponding IC_{20} and IC_{50} values were derived for the mixtures, with mixture concentration (c_{mix}) being expressed as the total molar concentration of TTR-binding compounds in proportions reflecting their median concentrations in maternal serum, infant serum, and house dust reported in Nordic countries. For the SRM2585 dust extract, concentration–response curves with corresponding IC_{20} and IC_{50} values were derived, expressed as the corresponding dust concentration in the assay (in grams of dust per liter).

Concentration–effect data analysis for individual compounds and mixtures was performed by a best-fit approach (Scholze et al. 2001) where various nonlinear regression models were fitted to the same pooled data set and the model that described data best was selected. In case of a significant inter-study data variation, experiment was included as random factor in the best-fit data analysis (nonlinear mixed effect model (see Altenburger et al. 2018 for more detail).

The effects of the reconstituted mixtures were predicted according to the principle of concentration addition (CA) under the assumption of noninteraction between the compounds (Greco et al. 1995). The concentration of the mixture causing $x\%$ inhibition (ICx_{mix}) is calculated from the ICx for each individual compound i (ICx_i) leading to the same response X and the relative molar contribution p_i of each compound i to the mixture (Faust et al. 2003):

$$ICx_{mix} = \left[\sum_{i=1}^{n} \left(\frac{p_i}{ICx_i} \right) \right]^{-1}. \tag{2}$$

If an ICx for the mixture could not be derived due to incomplete regression curves for the individual compounds (i.e., the individual compounds did not reach an $x\%$ inhibition level; Figure 1), a worst-case range of mixture predictions was estimated according to the dose extrapolation approach for CA predictions (Scholze et al. 2014). To account for the statistical uncertainty in the CA prediction, a combined Monte-Carlo (MC) and nonlinear regression bootstrap simulation was conducted to establish approximate 95% confidence limits around the predicted mean mixture response. For each compound a distribution of resampled model fits was simulated by parametric bootstrap with resamples drawn from the fitted nonlinear (mixed) effect model (Faust et al. 2003), which then was used as input for an MC to generate a distribution of mixture prediction. Differences between predicted and observed mixture effects were deemed statistically significant when the 95% confidence belts of the prediction did not overlap with those of the experimentally observed mixture effects.

Toxic Unit Summation

Under the assumption of CA, the ratio between the c_{mix} and the concentration of the mixture expected to cause $x\%$ inhibition (ICx_{mix}) is calculated by the method of Toxic Unit (TU) summation:

$$TU_{sum} = \frac{c_{mix}}{ICx_{mix}} = \sum_{i=1}^{n} TU_i = \sum_{i=1}^{n} \left(\frac{c_i}{ICx_i} \right), \tag{3}$$

with c_i being the concentration of the ith compound in the mixture ($c_{mix} = c_1 + \cdots + c_n$), TU_i representing the toxic unit of the ith compound ($TU_i = c_i/ICx_i$), and TU_{sum} representing the toxic units summation. If TU_{sum} equals 1, the mixture concentration is expected to produce $x\%$ inhibition; if it is smaller or greater, the observable inhibition should be smaller or greater, respectively, although no quantitative expectation on the effect size can be provided.

K_i Estimation

For each individual inhibitor, its IC_{20} value in the bioassay was converted into a K_i value (i.e., the dissociation constant of the inhibitor–TTR complex), according to

$$K_i = \frac{K_d \times [PL_{20}] \times IC_{20}}{[L_{20}] \times [PI_{20}]} - [P_{20}], \tag{4}$$

where $[PL_{20}]$ is the concentration of protein–ligand complex, which is 20% lower than in the absence of inhibitor, and with $[L_{20}]$, $[PI_{20}]$, $[P_{20}]$ being the corresponding concentrations of free ligand, protein–

inhibitor complex, and free protein, respectively. Derivation of Equation 4 and estimation of $[L_{20}]$, $[PI_{20}]$, and $[P_{20}]$ are described in detail in "S1.4 Derivation of K_i from the IC_x determined in the bioassay" in the Supplemental Material, based on Nikolovska-Coleska et al. (2004). The 20% inhibition level was chosen because robust IC_{20} values could be established for all compounds in the test set.

Similar K_i calculations were made for mixtures reflecting median or high-end concentrations in maternal and infant blood from Nordic countries (see Excel Tables S1 and S2). The underlying IC_{20} values of these mixtures in the bioassay were calculated based on concentration addition (Equation 2) using the molar proportions of the constituents in the different mixtures considered (see Table S2).

Extrapolation to Human Blood

The degree by which the different inhibitor mixtures inhibit FITC-T_4 binding to TTR *in vitro* cannot be directly translated into *in vivo* inhibition levels for TTR-T_4 binding in human blood, because the assay makes use of a fluorescent FITC-T_4 probe, and not T_4. Moreover, T_4 in human blood not only forms a protein–ligand complex with TTR, but also with other proteins, of which TBG and ALB have highest T_4-binding capacity (Salvatore et al. 2016).

In the absence of inhibitor, three protein–ligand equilibria are in place that determine the degree of T_4-TTR binding, that is,

$$K_d P = \frac{[L] \times [P]}{[PL]} \tag{5}$$

$$K_d X = \frac{[L] \times [X]}{[XL]} \tag{6}$$

$$K_d Y = \frac{[L] \times [Y]}{[YL]} \tag{7}$$

where
  $[L]$ is the concentration of free ligand (i.e., T_4 in blood);
  $[P]$, $[X]$, and $[Y]$ are the concentrations of unbound TTR, TBG, and ALB, respectively;
  $[PL]$, $[XL]$, and $[YL]$ are the concentrations of the protein–ligand complex TTR-T_4, TBG-T_4, and ALB-T_4, respectively;
  $K_d P$, $K_d X$, and $K_d Y$ are the dissociation constants of the protein–ligand complex for TTR, TBG, and ALB, respectively.

In the presence of inhibitor I, an additional equilibrium reaction is in place for the inhibitor–TTR complex, that is,

$$K_i P = \frac{[I] \times [P]}{[PI]} \tag{8}$$

where $K_i P$ is the dissociation constant of the protein–inhibitor complex for TTR, and $[I]$ and $[PI]$ are the concentrations of the free inhibitor and the inhibitor–TTR complex, respectively.

In addition to these four equilibrium reactions, the following five mass balances are in place:

$$[L_T] = [L] + [PL] + [XL] + [YL] \tag{9}$$

$$[P_T] = [P] + [PL] + [PI] \tag{10}$$

$$[X_T] = [X] + [XL] \tag{11}$$

$$[Y_T] = [Y] + [YL] \tag{12}$$

$$[I_T] = [I] + [PI] \tag{13}$$

with $[X_T]$, $[Y_T]$, and $[I_T]$ being the total concentration of ligand TBG, ALB, and inhibitor, respectively. For the known parameters in these equations, estimates for $[L_T]$, $[P_T]$, $[X_T]$, and $[Y_T]$ in pregnant women and infants and for human K_dX and K_dY were obtained as mean or median values reported in the literature (see Table S3), whereas estimates for K_dP and K_iP and for $[I_T]$ in maternal and infant blood were obtained from the present study (Tables 1 and 2, respectively). The remaining five unknown parameters (i.e., the free concentrations $[L]$, $[P]$, $[X]$, $[Y]$, and $[I]$)

were then estimated by solving the five mass balances after rearrangements of Equations 9–13 with Equations 5–8. The actual rearrangements as well as the method for solving the mass balances are described in detail in "S1.5 Extrapolation to human blood – Solving the five mass balances" in the Supplemental Material.

Finally, the inhibition level of T_4-TTR binding in human blood was determined by comparing the estimated $[PL]$ in the presence of the inhibitor mixture to the estimated $[PL]$ in the absence of inhibitor mixture (i.e., $[I_T] = 0$).
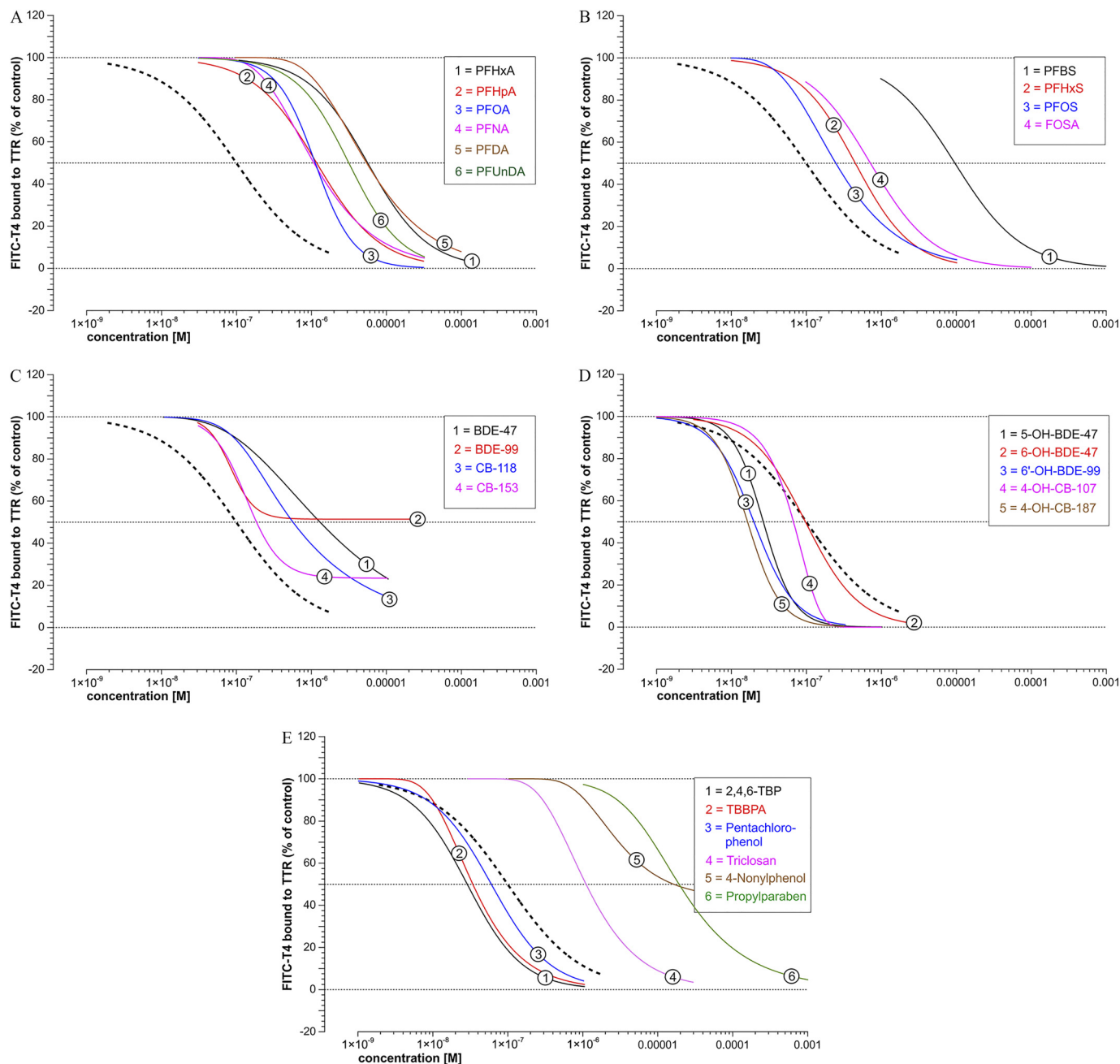
Figure 1. Individual concentration–response curves for the 25 selected test compounds in the FITC-T_4 TTR-binding assay. (A) Perfluoroalkyl carboxyl acids (PFCA); (B) perfluoroalkyl sulfonic acids (PFSAs) and FOSA; (C) PCBs and PBDEs; (D) PCB metabolites and PBDE metabolites; (E) other phenols and propylparaben. In each panel the concentration–response curve for the natural ligand T_4 is displayed as a dashed curve (---). Note: 2,4,6,-TBP, 2,4,6-tribromophenol; 4-OH-CB-107, 4-OH-2,3,3′,4′,5-pentachlorobiphenyl; 4-OH-CB-187, 4-OH-2,2′,3,4′,5,5′,6-heptachlorobiphenyl; 5-OH-BDE-47, 5-OH-2,2′,4,4′-tetrabromodiphenyl ether; 6-OH-BDE-47, 6-OH-2,2′,4,4′-tetrabromodiphenyl ether; 6′-OH-BDE-99, 6′-OH-2,2′,4,4′,5-pentabromodiphenyl ether; BDE-47, 2,2′,4,4′-tetrabromodiphenyl ether; BDE-99, 2,2′,4,4′,5-pentabromodiphenyl ether; CB-118, 2,3′,4,4′,5-pentachlorobiphenyl; CB-153, 2,2′,4,4′,5,5′-hexachlorobiphenyl; FITC, fluorescein 5-isothiocyanate; FOSA, perfluorooctane sulfonamide; PCB, polychlorinated biphenyl; PDBE, polybrominated diphenyl ether; PFBS, perfluorobutane sulfonic acid; PFDA, perfluorodecanoic acid; PFHpA, perfluoroheptanoic acid; PFHxA, perfluorohexanoic acid; PFHxS, perfluorohexane sulfonic acid; PFNA, perfluorononanoic acid; PFOA, perfluorooctanoic acid; PFOS, perfluorooctane sulfonic acid; PFUnDA, perfluoroundecanoic acid; T_4, thyroxine; TBBPA, tetrabromobisphenol-A; TTR, transthyretin.

Table 1. Concentration–response regression models for the displacement of FITC-T$_4$ from TTR by individual compounds, SRM2585 dust extract, and reconstituted mixtures.

Substance	RM	$\widehat{\beta}_1$	$\widehat{\beta}_2$	$\widehat{\beta}_3$	$\widehat{\beta}_{min}$	β_{max}	IC$_{20}$ (M)	[95% CI of IC$_{20}$]	IC$_{50}$ (M)	K_i (M)
					Concentration–response function[a]					
Thyroxine (T$_4$)	Logit	−14.3	−2.05		0[b]	1	2.1×10^{-8}	$[1.8 \times 10^{-8}, 2.5 \times 10^{-8}]$	1.0×10^{-7}	3.2×10^{-8c}
PFHxA	Logit	−13.2	−2.50		0[b]	1	1.6×10^{-6}	$[1.1 \times 10^{-6}, 2.1 \times 10^{-6}]$	5.6×10^{-6}	3.4×10^{-6}
PFHpA	Logit	−14.0	−2.36		0[b]	1	3.0×10^{-7}	$[2.4 \times 10^{-7}, 3.8 \times 10^{-7}]$	1.2×10^{-6}	6.4×10^{-7}
PFOA	Logit	−23.3	−3.91		0[b]	1	4.9×10^{-7}	$[3.2 \times 10^{-7}, 7.4 \times 10^{-7}]$	1.1×10^{-6}	1.1×10^{-6}
PFNA	Weibull	−11.1	−1.79		0[b]	1	3.6×10^{-7}	$[2.9 \times 10^{-7}, 4.5 \times 10^{-7}]$	1.1×10^{-6}	7.7×10^{-7}
PFDA	Weibull	−9.28	−1.69		0[b]	1	1.7×10^{-6}	$[1.4 \times 10^{-6}, 2.2 \times 10^{-6}]$	5.4×10^{-6}	3.7×10^{-6}
PFUnDA	Logit	−15.6	−2.84		0[b]	1	1.0×10^{-6}	$[6.1 \times 10^{-7}, 1.6 \times 10^{-6}]$	3.1×10^{-6}	2.2×10^{-6}
PFBS	Logit	−11.2	−2.24		0[b]	1	2.3×10^{-6}	$[1.7 \times 10^{-6}, 3.3 \times 10^{-6}]$	9.7×10^{-6}	5.1×10^{-6}
PFHxS	Logit	−16.7	−2.63		0[b]	1	1.4×10^{-7}	$[9.7 \times 10^{-8}, 1.9 \times 10^{-7}]$	4.6×10^{-7}	2.8×10^{-7}
PFOS	Weibull	−11.8	−1.73		0[b]	1	8.2×10^{-8}	$[6.2 \times 10^{-8}, 1.1 \times 10^{-7}]$	2.5×10^{-7}	1.6×10^{-7}
FOSA	Logit	−14.6	−2.38		0[b]	1	1.9×10^{-7}	$[1.3 \times 10^{-7}, 2.7 \times 10^{-7}]$	7.3×10^{-7}	4.0×10^{-7}
Propylparaben	G.logit I	−16.3	−3.18	0.454	0[b]	1	5.5×10^{-6}	$[3.8 \times 10^{-6}, 7.2 \times 10^{-6}]$	1.9×10^{-5}	1.2×10^{-5}
4-Nonylphenol	Weibull	−12.7	−2.21		0.433	1	1.8×10^{-6}	$[1.2 \times 10^{-6}, 2.7 \times 10^{-6}]$	1.6×10^{-5}	3.9×10^{-6}
Pentachlorophenol	Logit	−18.4	−2.55		0[b]	1	1.7×10^{-8}	$[1.1 \times 10^{-8}, 2.8 \times 10^{-8}]$	6.0×10^{-8}	2.4×10^{-8}
Triclosan	Weibull	−12.7	−2.08		0[b]	1	4.4×10^{-7}	$[3.4 \times 10^{-7}, 5.9 \times 10^{-7}]$	1.1×10^{-6}	9.3×10^{-7}
TBBPA	Weibull	−17.0	−2.23		0[b]	1	1.4×10^{-8}	$[1.2 \times 10^{-8}, 1.8 \times 10^{-8}]$	3.4×10^{-8}	1.7×10^{-8}
2,4,6-TBP	Logit	−20.5	−2.71		0[b]	1	8.9×10^{-9}	$[6.9 \times 10^{-9}, 1.1 \times 10^{-8}]$	2.9×10^{-8}	5.5×10^{-9}
BDE-47	G.logit II	−20.2	−1.07	7.74×10^5	0[b]	1	2.1×10^{-7}	$[1.4 \times 10^{-7}, 3.1 \times 10^{-7}]$	1.3×10^{-6}	4.4×10^{-7}
5-OH-BDE-47	Logit	−36.9	−4.87		0[b]	1	1.4×10^{-8}	$[8.7 \times 10^{-9}, 2.1 \times 10^{-8}]$	2.7×10^{-8}	1.6×10^{-8}
6-OH-BDE-47	Logit	−19.7	−2.8		0[b]	1	3.1×10^{-8}	$[2.4 \times 10^{-8}, 4.2 \times 10^{-8}]$	9.8×10^{-8}	5.4×10^{-8}
BDE-99	Logit	−44.5	−6.29		0.514	1	7.3×10^{-8}	$[5.6 \times 10^{-8}, 8.9 \times 10^{-8}]$	—[g]	1.5×10^{-7}
6′-OH-BDE-99	Logit	−28.3	−3.68		0[b]	1	8.4×10^{-9}	$[5.5 \times 10^{-9}, 1.2 \times 10^{-8}]$	2.0×10^{-8}	4.5×10^{-9}
CB-118	G.logit I	−32.8	−4.72	0.209	0[b]	1	1.6×10^{-7}	$[1.2 \times 10^{-7}, 2.0 \times 10^{-7}]$	5.6×10^{-7}	3.2×10^{-7}
4-OH-CB-107	G.logit I	−14.7	−3.71	1.04×10^5	0[b]	1	3.4×10^{-8}	$[2.5 \times 10^{-8}, 4.5 \times 10^{-8}]$	6.8×10^{-8}	5.9×10^{-8}
CB-153	Logit	−30.6	−4.45		0.234	1	7.7×10^{-8}	$[6.3 \times 10^{-8}, 9.2 \times 10^{-8}]$	1.8×10^{-7}	1.5×10^{-7}
4-OH-CB-187	Logit	−35.4	−4.55		0[b]	1	8.2×10^{-9}	$[5.4 \times 10^{-9}, 1.2 \times 10^{-8}]$	1.7×10^{-8}	4.0×10^{-9}
SRM2585	Logit	−1.19	−2.13		0[b]	1	6.2×10^{-2d}	$[4.1 \times 10^{-2}, 8.9 \times 10^{-2}]^d$	2.8×10^{-1d}	NA[e]
Mixtures										
Maternal	Logit	−18.9	−2.72		0[b]	1	3.7×10^{-8}	$[2.5 \times 10^{-8}, 5.4 \times 10^{-8}]$	1.8×10^{-7f}	6.7×10^{-8}
Infant	Logit	−19.2	−2.75		0[b]	1	3.3×10^{-8}	$[2.4 \times 10^{-8}, 4.4 \times 10^{-8}]$	1.3×10^{-7f}	5.7×10^{-8}
House dust	Logit	−14.9	−2.50		0[b]	1	3.2×10^{-7}	$[2.2 \times 10^{-7}, 4.6 \times 10^{-7}]$	1.5×10^{-6f}	6.8×10^{-7}

Note: 2,4,6,-TBP, 2,4,6-tribromophenol; 4-OH-CB-107, 4-OH-2,3,3′,4′,5-pentachlorobiphenyl; 4-OH-CB-187, 4-OH-2,2′,3,4′,5,5′,6-heptachlorobiphenyl; 5-OH-BDE-47, 5-OH-2,2′,4,4′-tetrabromodiphenyl ether; 6-OH-BDE-47, 6-OH-2,2′,4,4′-tetrabromodiphenyl ether; 6′-OH-BDE-99; 6′-OH-2,2′,4,4′,5-pentabromodiphenyl ether; BDE-47, 2,2′,4,4′-tetrabromodiphenyl ether; BDE-99, 2,2′,4,4′,5-pentabromodiphenyl ether; CB-118, 2,3′,4,4′,5-pentachlorobiphenyl; CB-153, 2,2′,4,4′,5,5′-hexachlorobiphenyl; CI, confidence interval; FITC, fluorescein 5-isothiocyanate; FOSA, perfluorooctane sulfonamide; IC$_{20}$, 20% inhibitory concentration; IC$_{50}$, 50% inhibitory concentration; K_i, protein–inhibitor dissociation constant; NA, not applicable; PFBS, perfluorobutane sulfonic acid; PFDA, perfluorodecanoic acid; PFHpA, perfluoroheptanoic acid; PFHxA, perfluorohexanoic acid; PFHxS, perfluorohexane sulfonic acid; PFNA, perfluorononanoic acid; PFOA, perfluorooctanoic acid; PFOS, perfluorooctane sulfonic acid; PFUnDA, perfluoroundecanoic acid; RM, regression model; SRM2585, Standard Reference Material® 2585 house dust extract; T$_4$, thyroxine; TBBPA, tetrabromo-bisphenol-A; TTR, transthyretin.

[a]Mathematical regression model as defined by Scholze et al. (2001): $\widehat{\beta}_1, \widehat{\beta}_2, \widehat{\beta}_3, \widehat{\beta}_{min}$ estimated model parameters, given for concentrations expressed in M (rounded values), β_{max} were not estimated, but set to 1 relating to the mean value of the controls.

[b]Held fixed.

[c]The dissociation constant for the TTR-T$_4$ complex was determined as a K_i value for T$_4$ in the competitive binding experiments with ligand FITC-T$_4$ and competitor T$_4$ but was applied as a K_d value for T$_4$ in the extrapolation from the *in vitro* bioassay to the *in vivo* situation in human blood.

[d]IC$_{20}$ and IC$_{50}$ values for the SRM2585 house dust sample are expressed in g dust/L, not in M.

[e]The K_i value for house dust cannot be calculated given that it should be expressed in mol/L, not in g/L.

[f]Derived from the toxic unit extrapolation method by Scholze et al. (2014): the two worst-case toxic unit assumptions resulted into nearly identical estimation and thus are reported only as single value.

[g]50% inhibition level was not reached for BDE-99 (see Figure 1).

Contribution of Test Compounds to TTR-Binding Potency of Dust

For 16 of the 25 compounds tested in this study, a concentration q_i (mol/g dust) in the SRM2585 dust sample could be retrieved from the NIST Certificate of Analysis (NIST 2018), and from open literature (see Table S4). For each of these 16 compounds, its TTR-binding potency in the FITC-T$_4$ binding assay relative to T$_4$ was expressed as a relative effect potency (REP_i) according to

$$REP_i = \frac{IC20_{T4}}{IC20_i}. \qquad (14)$$

The combined TTR-binding potency of the 16 contaminants in the SRM2585 sample was expressed as a calculated T$_4$-equivalent concentration in dust [$qT4EQ_{calculated}$] (mol/g dust) by

$$[qT4EQ_{calculated}] = \sum_{i=1}^{16}(q_i \times REP_i). \qquad (15)$$

Upon testing its extract in the FITC-T$_4$ binding assay, the TTR-binding potency of the SRM2585 dust sample was expressed as $IC20_{dust}$, that is, the dust concentration (g dust/L) corresponding to the extract concentration causing 20% inhibition in the assay. $IC20_{dust}$ was converted into a T$_4$-equivalent concentration in dust [$qT4EQ_{test}$] (mol/g dust) according to

$$[qT4EQ_{test}] = \frac{IC20_{T4}}{IC20_{dust}}. \qquad (16)$$

Finally, the contribution of the 16 compounds to the overall TTR-binding potency of the SRM2585 extract was determined by comparing [$qT4EQ_{calculated}$] to [$qT4EQ_{test}$].

Results

Mixture Composition

To design a mixture that reflects the composition of TTR-binding contaminants in house dust, infant serum, and maternal serum,

Table 2. Total concentrations and corresponding TTR-binding potencies of mixtures consisting of median or high-end concentrations determined in maternal and infant serum from Nordic countries as measured in the *in vitro* binding assay and as extrapolated to human blood.

Parameter	Maternal mixture based on		Infant mixture based on	
	Median concentrations	High-end concentrations	Median concentrations	High-end concentrations
Total inhibitor concentration in blood (M)	5.1×10^{-8}	2.5×10^{-7}	4.0×10^{-8}	1.3×10^{-7}
IC_{20} predicted in bioassay (M)	5.7×10^{-8}	7.3×10^{-8}	3.9×10^{-8}	3.1×10^{-8}
(95% confidence interval)	$[4.2 \times 10^{-8}, 7.2 \times 10^{-8}]$	$[5.3 \times 10^{-8}, 9.5 \times 10^{-8}]$	$[2.7 \times 10^{-8}, 5.5 \times 10^{-8}]$	$[2.1 \times 10^{-8}, 4.5 \times 10^{-8}]$
TU_{sum} in blood based on IC_{20} in bioassay	0.89	3.5	1.0	4.0
K_i (predicted in the bioassay) (M)	1.1×10^{-7}	1.5×10^{-7}	7.1×10^{-8}	5.4×10^{-8}
Fraction of TTR in blood occupied by T_4 (%)				
Without inhibitor mixture	0.11	0.11	0.085	0.085
With inhibitor mixture	0.10	0.099	0.084	0.081
Fraction of T_4 in blood bound to TTR (%)				
Without inhibitor mixture	3.1	3.1	1.7	1.7
With inhibitor mixture	3.0	2.9	1.7	1.6
Inhibition in T_4-TTR binding in blood compared with situation without inhibitor mixture (%)[a]	1.3	6.2	1.5	4.9
IC_{20} in blood (M)	8.0×10^{-7}	8.1×10^{-7}	5.2×10^{-7}	5.1×10^{-7}
TU_{sum} in blood based on IC_{20} in blood	0.063	0.31	0.077	0.24
Margin of exposure to IC_{20} in blood	16	3.2	13	4.1

Note: All estimates are based on predicted IC_{20} values calculated according to the principle of concentration addition. The corresponding estimates for the different blood parameters used to make these calculations (i.e., total levels of T_4, TTR, TBG, ALB, and K_d values for the T_4-TTR, T_4-TBG, and T_4-ALB complexes) are provided in Table S3. ALB, albumin; CI, confidence interval; IC_{20}, 20% inhibitory concentration; K_i, protein–inhibitor dissociation constant; T_4, thyroxine; TBG, thyroid hormone binding globulin; TTR, transthyretin; TU_{sum}, Toxic Unit summation.
[a]See Figure 4.

median concentrations of the test compounds in these three different matrices were collected from the open literature from studies performed in Sweden or alternatively in a European, preferably Nordic, country (see Excel Tables S1 and S2). Median concentrations in house dust could be collected for 18 of the 25 selected compounds (see Excel Table S1). This excluded the five hydroxylated PBDE and PCB metabolites, which are not expected to be found in house dust, and FOSA and nonylphenol, which have been reported in Swedish serum but had very low detection frequency in European house dust. Median concentrations in human serum were collected for 22 compounds, that is, 21 in maternal serum and 20 in infant serum (see Excel Table S1). No median human serum levels could be retrieved for PFHxA, PFUnDA, and PFBS from Swedish, Nordic, or European studies. At the time of performing the literature search, very few studies had actually looked for these PFASs in human serum. Therefore, it was decided to include these three compounds in the dust mixture to address a more complete PFAS exposure profile to humans.

Mixtures reflecting median concentrations in house dust, maternal, and infant serum were dominated by only a few of the test compounds. In fact, >80% of the molar mixture composition could be attributed to 2 of 18 compounds in the reconstituted dust mixture (i.e., propylparaben and triclosan), 4 of 21 compounds in the reconstituted maternal serum mixture (i.e., PFHxS, PFOS, pentachlorophenol, and PFOA), and 3 of 20 compounds in the reconstituted infant serum (i.e., PFOS, pentachlorophenol, and PFOA). Compositions of the reconstituted maternal and infant serum mixtures were similar, and differed considerably from the house dust mixture. The exact compositions of the reconstituted mixtures tested in the TTR-binding assay are provided in Table S1.

### TTR-Binding by Individual Compounds

From the saturation experiment with 30 nM TTR and a concentration series of FITC-T_4, a K_d value of 140 nM was determined for the FITC-T_4-TTR complex. For all individual test compounds a concentration-dependent displacement of FITC-T_4 from the TTR protein was observed in the competitive binding experiments (Figure 1), confirming earlier studies with a radioligand binding assay (RLBA) (see Excel Table S1). All concentration–response models as well as the estimates for their IC_{20}, IC_{50}, and

K_i values are provided in Table 1. As was to be expected based on structural similarities with T_4 and on previously reported RLBA results, 2,4,6-TBP, pentachlorophenol, TBBPA (Figure 1E), and the metabolites of PBDEs and PCBs (Figure 1D) had the highest competitive potency to displace FITC-T_4 from the TTR protein. In fact, these halogenated phenols all had higher competitive binding potencies than the endogenous ligand T_4 itself. The PFASs had TTR-binding potencies lower than T_4 (Figure 1A,B), with the highest potencies found for PFOS. Remarkably, the parent PBDE and PCB compounds also showed competitive binding to TTR, but at high test concentrations the maximum competitive potency of BDE-99 and PCB-153 leveled off before reaching complete inhibition (Figure 1C). In the RLBA, only very weak TTR-binding potency had been observed for the parent PBDE and PCB compounds. Altogether, a Pearson's correlation coefficient of $r = 0.87$ was observed between log-transformed IC_{50} values determined in the competitive binding assay with FITC-T_4 (the present study) and log-transformed IC_{50} values previously reported (see Excel Table S1) for the competitive binding assay with radiolabeled T_4 (see Figure S1).

TTR-Binding by Reconstituted Mixtures

For all three mixtures, a concentration-dependent decrease in TTR-binding by FITC-T_4 was observed, reaching 100% displacement at the highest test concentrations (Figure 2). For each mixture, the concentration–response curve fitted on the measured data overlapped with the confidence intervals of the concentration–response curve calculated according to concentration addition, indicating that TTR-binding of complex mixtures can indeed be approximated well by the concentration addition principle.

The combined median concentrations actually reported in maternal or infant serum from Nordic countries approached the IC_{20} determined for the experimentally tested mixtures (i.e., $TU_{sum} \approx 1$) (Figures 2 and 3; Table 2). According to the principle of concentration addition, concentration response curves and corresponding IC_{20} values were calculated for the nontested mixtures reflecting high-end concentrations in maternal and infant serum. For these mixtures, the combined high-end concentrations exceeded the predicted IC_{20} in the bioassay by a factor >3 (i.e., $TU_{sum} = 3.5$ and $TU_{sum} = 4.0$ for the maternal and infant mixture, respectively; Table 2).
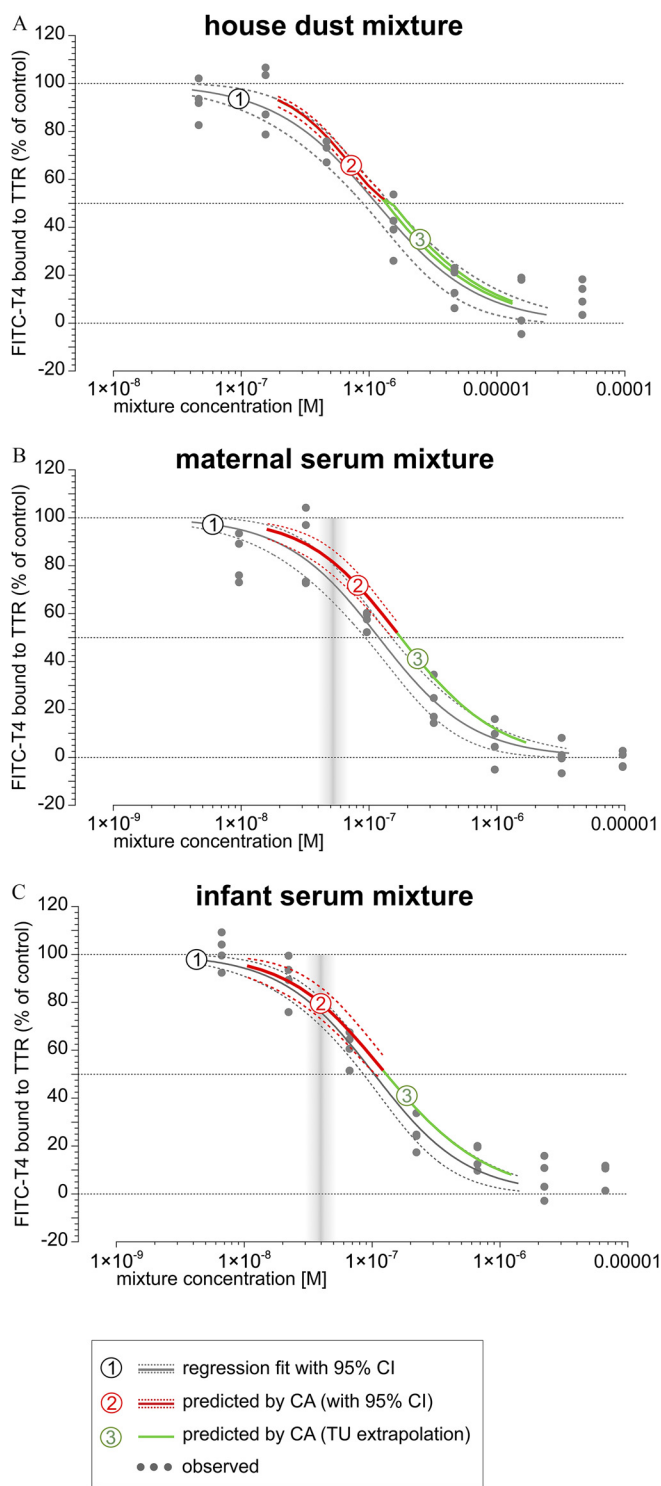
Figure 2. Concentration–response curves for the reconstituted mixtures based on the ratio of median concentrations reported in (A) house dust, (B) maternal serum, and (C) infant serum from Nordic countries. The vertical gray bar in plots B and C indicates the mixture concentration reflecting the median concentration of the individual compounds actually detected in maternal or infant blood samples from Nordic countries. Note: CA, concentration addition; CI, confidence interval; FITC, fluorescein 5-isothiocyanate; T_4, thyroxine; TTR, transthyretin; TU, Toxic Unit.

More than 80% of the inhibition caused by the reconstituted house dust mixture could be attributed to 5 of the 18 compounds present in the mixture, that is, triclosan, TBBPA, BDE-99, pentachlorophenol, and 2,4,6-TBP. For the reconstituted maternal and infant serum mixtures this was the case for even fewer compounds, that is, 3 of 21 (pentachlorophenol, PFOS, and PFHXs) and 2 of 20 compounds (pentachlorophenol and PFOS), respectively (see Figure 3).

TTR-Binding by House Dust Extract

For the 16 compounds tested in the present study and analyzed in the SRM2585 dust sample, a summarized T_4-equivalent concentration was calculated of 4.0 nmol/g dust (see Table S4). In the TTR-binding assay, the SRM2585 extract showed a concentration-dependent displacement of FITC-T_4, with $IC20_{dust} = 0.062$ g dust/L (Table 1). Using the IC_{20} for T_4 (Table 1), the T4EQ concentration of the SRM2585 dust sample was estimated to be $21/0.062 = 340$ nmol/g dust (Equation 16). Consequently, the 16 compounds for which concentrations were available could only explain $4.0/340 = 1.2\%$ of the totally measured TTR-binding potency.

Extrapolation to Human Blood

Using the dissociation constants for the T_4-TTR ligand–protein complex (Table 1; this study) and for the T_4-TBG and T_4-ALB ligand–protein complexes as well as the median or mean total T_4 levels determined in normal adult, maternal, or infant blood reported in literature (see Table S3), >99% of the total T_4 concentration in human blood was calculated to bind to the TH binding proteins in the absence of inhibitors. The corresponding TTR/TBG/ALB distribution was estimated to be 6/76/18% in normal adult blood. During the first trimester of pregnancy, when the fetus depends completely on the maternal TH supply, the calculated TTR/TBG/ALB distribution in maternal blood shifts in the direction of TBG (i.e., 3/87/10%), due to increased TBG levels and decreased TTR and ALB levels compared with normal levels (see Table S3). Also for infants, the calculated TTR/TBG/ALB distribution is more dominated by TBG than in normal adults (i.e., 4/90/6%), due to higher TBG and lower TTR and ALB concentrations than reported for normal adults (see Table S3).

In maternal blood, the mixture of inhibitors reflecting median concentrations was estimated to cause a 1.3% inhibition in T_4-TTR binding compared with the uninhibited situation. In infant blood, the median mixture of inhibitors was estimated to cause a 1.5% inhibition in T_4-TTR binding (Table 2; Figure 4). At high-end inhibitor concentrations, 6.2% inhibition was estimated in maternal blood and 4.9% in infant blood. Consequently, the median or high-end concentrations in maternal or infant blood were lower than the inhibitor concentrations expected to cause 20% *in vivo* inhibition in human blood (i.e., $TU_{sum} < 1$), but margins of exposure were small, ranging from 13 to 16 for median concentrations and from 3.2 to 4.1 for high-end concentrations (Table 2).

Discussion

The goal of the present study was to determine the TTR-binding potency of reconstituted mixtures of house dust contaminants as present in maternal serum, infant serum, and house dust. In addition, we investigated whether this potency could be predicted according to the principle of concentration addition. Similar TTR-binding potencies were observed for the mixtures reflecting median concentrations in maternal and infant serum in terms of IC_{20} values (37 and 33 nM, respectively), IC_{50} values (180 and 130 nM), and corresponding K_i values (67 and 57 nM). The house dust mixture was less potent (i.e., $IC_{20} = 320$ nM, $IC_{50} = 1.5$ μM, $K_i = 680$ nM), due to differences in composition between both serum and house dust mixtures (see Table S1).

A major part (i.e., >80%) of the observed inhibition of FITC-T_4 binding to TTR could be attributed to a minor part (i.e., <20%)
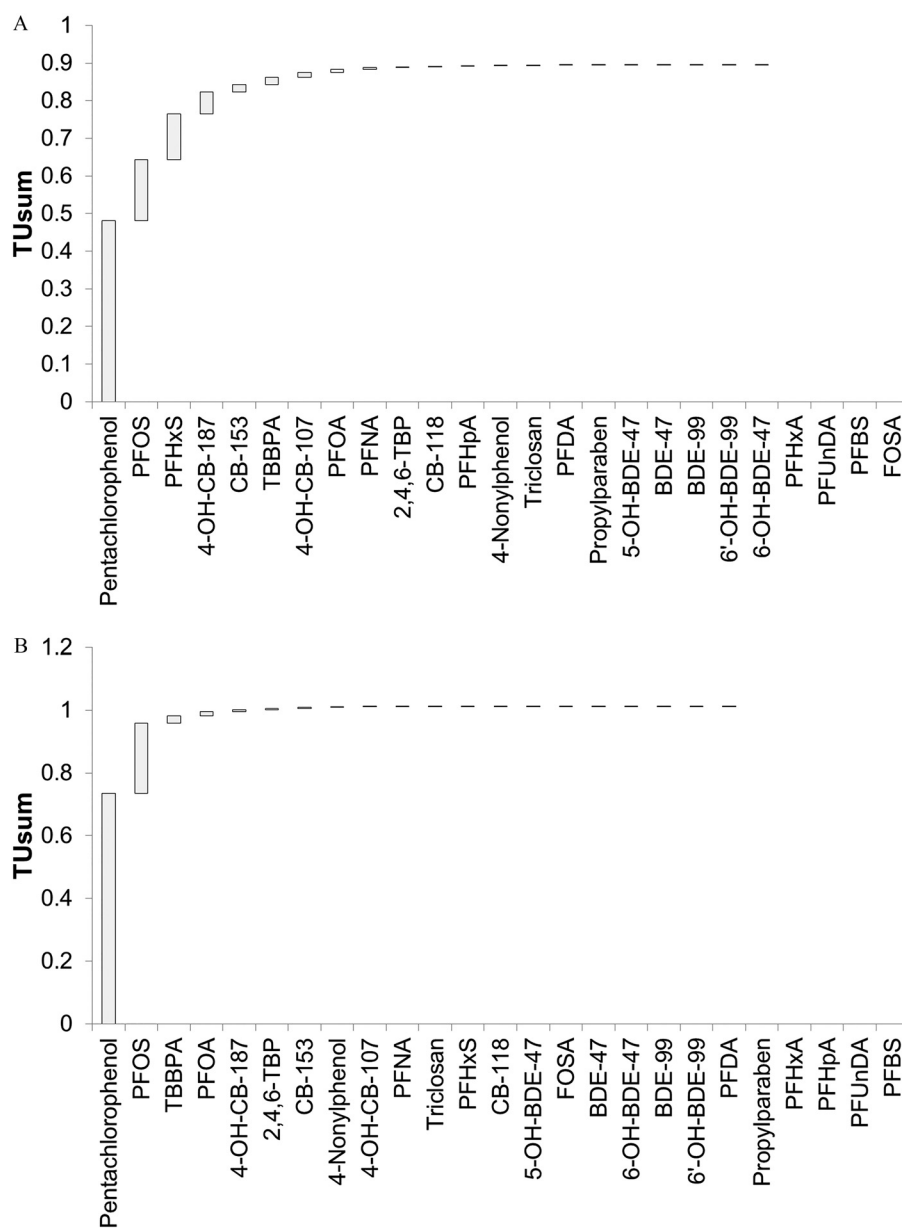
Figure 3. Cumulative plots showing the predicted TTR-binding potency of house dust contaminants or their metabolites at median concentrations reported in (A) maternal and (B) infant serum in Nordic countries. Compounds are ranked according to their contribution to the total TTR-binding potency of the mixture, predicted on the basis of the concentration addition principle. The y-axes represent the Toxic Unit summation (TU_{sum}), i.e., the sum of ranked ratios of the compounds' concentration and its IC_{20} value. Note: 2,4,6,-TBP, 2,4,6-tribromophenol; 4-OH-CB-107, 4-OH-2,3,3′,4′,5-pentachlorobiphenyl; 4-OH-CB-187, 4-OH-2,2′,3,4′,5,5′,6-heptachlorobiphenyl; 5-OH-BDE-47, 5-OH-2,2′,4,4′-tetrabromodiphenyl ether; 6-OH-BDE-47, 6-OH-2,2′,4,4′-tetrabromodiphenyl ether; 6′-OH-BDE-99; 6′-OH-2,2′,4,4′,5-pentabromodiphenyl ether; BDE-47, 2,2′,4,4′-tetrabromodiphenyl ether; BDE-99, 2,2′,4,4′,5-pentabromodiphenyl ether; CB-118, 2,3′,4,4′,5-pentachlorobiphenyl; CB-153, 2,2′,4,4′,5,5′-hexachlorobiphenyl; FOSA, perfluorooctane sulfonamide; IC_{20}, 20% inhibitory concentration; PFBS, perfluorobutane sulfonic acid; PFDA, perfluorodecanoic acid; PFHpA, perfluoroheptanoic acid; PFHxA, perfluorohexanoic acid; PFHxS, perfluorohexane sulfonic acid; PFNA, perfluorononanoic acid; PFOA, perfluorooctanoic acid; PFOS, perfluorooctane sulfonic acid; PFUnDA, perfluoroundecanoic acid; TBBPA, tetrabromo-bisphenol-A; TTR, transthyretin.

of the compounds present in the mixture. These results support Pareto's principle that 80% of the outcome can be explained by only 20% (or less) of the causal factors. Similar results were previously found in an androgen-receptor (AR) antagonistic reporter gene assay with mixtures consisting of 22 anti-androgenic compounds that were reconstituted according to their proportion in average and high-end serum levels (Kortenkamp et al. 2014). In our TTR-binding assay, pentachlorophenol and TBBPA were driving compounds (i.e., explaining a significant amount of the observed TTR-binding capacity) in all three mixtures. Some compounds, however, were driving the TTR-binding potency in one reconstituted mixture but not in the other, like PFOS in both human serum mixtures, PFHxS and 4-OH-CB-187 more particular in the maternal serum mixture, and triclosan and propylparaben in the house dust mixture.

For the mixtures based on median blood levels, the actual median concentrations in blood were in the same range as the corresponding IC_{20} values determined in the bioassay (i.e., $TU_{sum} \approx 1$). In previous studies, the OH-PBDEs in blood from children working on Nicaraguan e-waste sites were estimated to contain TTR-binding
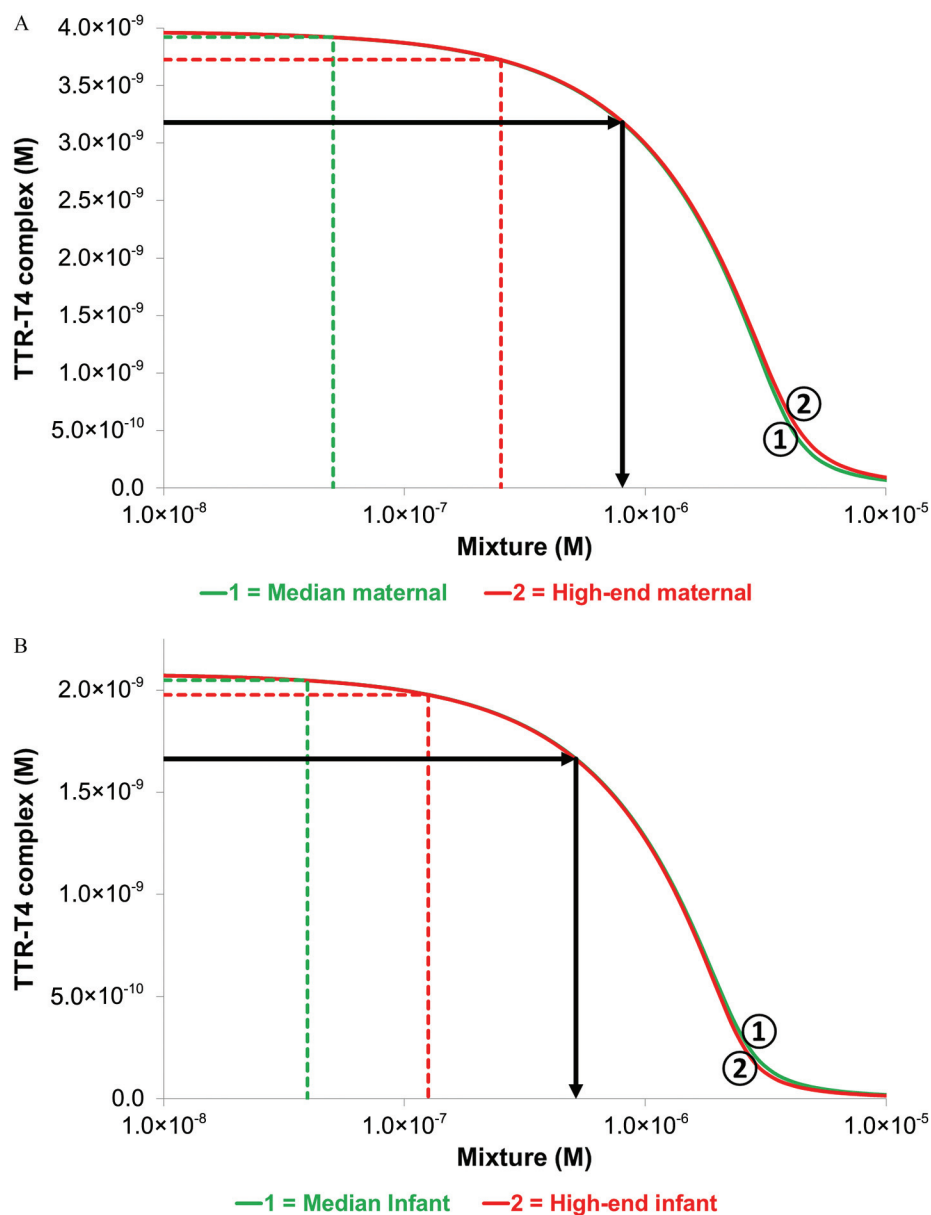
Figure 4. Estimated concentration–response curves in human blood for mixtures representing median concentrations or high-end concentration of house dust contaminants reported in human (A) maternal or (B) infant serum from Nordic countries. The vertical dashed lines indicate the actual median (left) and high-end (right) concentration found in serum, and the corresponding horizontal dashed lines indicate the concentration of the TTR-T_4 complex (top and bottom represent median and high-end respectively). The black arrows indicate the IC_{20} level estimated for serum, which overlap for the two dose–response curves in both panels, i.e., 8.0×10^{-7} M (median) and 8.1×10^{-7} M (high-end) for the maternal mixtures and 5.2×10^{-7} M (median) and 5.1×10^{-7} M (high-end) for the infant mixtures (Table 2). IC_{20}, 20% inhibitory concentration; T_4, thyroxine; TTR, transthyretin.

potency equivalent to 0.55 nM T_4 (Hamers et al. 2008). Similarly, the PFAS compounds in blood from European and North American adults were estimated to have TTR-binding potency equivalent to 3.1 and 5.1 nM T_4, respectively (Weiss et al. 2009). Given the IC_{20} of approximately 30 nM determined for T_4 in the radioligand binding assay used in these studies, the observed T_4 equivalent concentrations correspond to $TU_{sum} = 0.018$ for OH-PBDEs and to $TU_{sum} = 0.10$ to 0.17 for PFAS. These values are very much in line with the contribution of these compounds to the overall TTR-binding capacity determined in the present study (Figure 3).

The mixtures reflecting actual high-end concentrations in maternal and infant blood exceeded the IC_{20} predicted for the bioassay by a factor of 3.5 and 4.0, respectively. The relatively small difference in toxic potencies between the median and the high-end concentration mixtures is due to the fact that no maximum

concentrations were reported for many compounds. Instead, we used the 95th percentile from reported serum concentrations as a proxy for the maximum concentration, which implies that 5% of the population is expected to have even higher serum concentrations. For the PFAS compounds, high-end concentrations in maternal serum were estimated using a conservative ratio between the maximum and an average level of 3, based on PFAS measurements in a Spanish study (Manzano-Salgado et al. 2015). Altogether, ratios between high-end and median concentrations for most TTR-binding compounds ranged from <2 to 10, except for triclosan (both maternal and infant); PFHxS, PFOS, and TBBPA (infant); and propylparaben (maternal) (see Excel Tables S1 and S2).

The finding that median concentrations in blood correspond to IC_{20} levels in the bioassay cannot be directly translated to the actual *in vivo* inhibition of T_4-TTR binding in human blood at similar

inhibitor concentrations. After all, the bioassay makes use of a fluorescent-labeled FITC-T_4 probe (and not T_4 itself), which is tested in an overdose (i.e., $[\text{FITC-}T_4] = 110$ nM) compared with the only TH binding protein present in the assay (i.e., $[\text{TTR}] = 30$ nM). Under physiological conditions, T_4 is indeed present at similar concentrations as FITC-T_4 in the assay, but TTR is complemented by two other T_4-binding proteins (i.e., TBG and ALB), whereas all three T_4-binding proteins are present at much higher concentrations than the TTR concentration in the bioassay [see Table S3]. Using values from the literature for T_4 concentration and dissociation constants, [i.e., $[T_4] = 107$ nM, $K_d(\text{TTR}) = 14.3$, $K_d(\text{TBG}) = 0.100$, $K_d(\text{ALB}) = 1{,}430$ nM (Salvatore et al. 2016)], a 12/71/17% distribution of T_4 over TTR/TBG/ALB was calculated. This distribution is very similar to the 11/74/15% distribution calculated by Schussler (2000) based on free T_4 rather than total T_4 concentrations and to the 15/75/10% distribution traditionally believed to be present in blood (e.g., Richardson 2007), although it is unclear whether this latter distribution was actually calculated or measured. Using the dissociation constant determined in the present study for the TTR-T_4 complex (i.e., $K_d = 32$ nM; Table 1), however, the distribution of T_4 over TTR/TBG/ALB in blood was calculated to be 6/76/18%. The difference between both dissociation constants for the TTR-T_4 complex reported in the literature and determined in the present study may be due to differences in experimental temperatures, that is, 37°C (Robbins and Edelhoch 1986) and 4°C (the present study), although temperature did not seem to affect the T_4 binding in our binding assay (see Figure S2). The 4°C temperature was chosen in order to resemble previous studies with radioligand binding assays performed at this temperature (e.g., Hamers et al. 2008; Weiss et al. 2009; Zhang et al. 2015). Alternatively, the difference may be explained by the different methods used to establish the dissociation constant. Although the method used to determine the $K_d = 14.3$ nM is not clear, it must be different from the method used in the present study given that the fluorescent FITC-T_4 probe was not described before 2012 (Ren and Guo 2012). Still, both K_d values fit very well within the span of other K_d values reported in the literature ranging from $K_d = 5$ nM determined at unknown temperature (Feldt-Rasmussen and Rasmussen 2007) to $K_d = 84$ nM determined at 25°C (Purkey et al. 2001). Therefore, we have used the K_d value determined in the present study to estimate the *in vivo* inhibition for the human situation. Thus, the dissociation constant for the TTR-T_4 complex was directly comparable to the dissociation constant for the inhibitor–TTR complex determined at the same temperature (4°C).

Using these latter dissociation constants (i.e., K_i values), T_4-binding to TTR in blood was estimated to be inhibited by 1.3–1.5% by the mixture of house dust contaminants at median concentration levels (Table 2). The relevance of this T_4 displacement from TTR in humans remains to be clarified. For the majority of the TTR-binding compounds considered in the present study, rodent studies have found a decrease in circulating total T_4 levels in serum or plasma (see, for instance, reviews by EFSA 2005, 2011b, 2011a, 2018). The decrease is attributed to the fact that T_4 displaced from TTR is freely available for hepatic uptake and conjugation followed by biliary elimination. This increased hepatic clearance is further enhanced by the fact that many of the test compounds can activate nuclear CAR and PXR receptors, causing an induction of hepatic phase II enzymes responsible for glucuronidation or sulfation of T_4. Animal studies with PBDEs, PCBs, and PFASs have further indicated that decreased maternal levels of circulating T_4 are associated with neurodevelopmental effects on cognitive function, motor activity, and behavior in offspring (EFSA 2005, 2011b, 2011a, 2018). In humans, however, the situation is less clear. For the compounds considered in the present study, some studies have reported negative associations with T_4 levels in blood (DH Kim et al. 2016; Makey et al. 2016;

Zheng et al. 2017; Zota et al. 2011), but other studies have reported positive associations (EFSA 2011a; Shrestha et al. 2017; Stapleton et al. 2011), concentration-dependent associations (Zhao et al. 2015), or a lack of associations (Audet-Delage et al. 2013; Kato et al. 2016; Olsen et al. 2003). The observed difference between rodent and human studies is attributed to the fact that humans have a reserve of T_4 stably bound to TBG. In rodents, however, TBG is not found at the age they are usually tested for in animal studies (Lewandowski et al. 2004; Vranckx et al. 1990). As a consequence, rodents have a faster T_4 turnover than humans [half-life times of 12–24 h compared with 5–9 d, respectively (Jahnke et al. 2004)] and are considered to be more sensitive than humans to changes in TH balance by T_4 displacement from TTR or by induced hepatic clearance.

The higher binding affinity of T_4 for TBG than for TTR and ALB, which is also reflected by the TTR/TBG/ALB binding proportions calculated above, could be taken to suggest that TTR-binding in human blood is much less important than TBG-binding. This suggestion, however, is too simplistic because the actual relevance of TTR-binding is most likely not in the circulation of T_4 but in the delivery of free T_4 hormone to the target cells, which depends on the dissociation rate (k_{off}) of the TTR-T_4 complex and the capillary transit time (Richardson 2007). The dissociation rates for T_4 from the different TH binding proteins range from $k_{\text{off}} = 0.017$ s^{-1} for TBG, via $k_{\text{off}} = 0.080$ s^{-1} for TTR, to $k_{\text{off}} > 0.5$ s^{-1} for ALB (Mendel et al. 1988). Given the capillary transit time in different tissues (Mendel 1989), the contribution of the TTR-T_4 complex to the free T_4 pool equals that of the TBG-T_4 complex (Robbins 2002). As such, the late Sidney Ingbar, a specialist in thyroid endocrinology, considered TBG as the saving account for T_4 and TTR as the checking account (Robbins 2002). In the same context, others drew a parallel to the Goldilocks principle, that is, TBG binds T_4 too tightly for delivery of free T_4 to target cells, ALB binds T_4 too loosely, and TTR binds T_4 just right (Alshehri et al. 2015). Consequently, inhibition of TTR-T_4 binding by xenobiotic compounds may interfere with the level of T_4 delivery at the target tissue.

TTR is also known to play a role in the T_4 transport across at least two barriers in distribution, that is, the placenta and the blood-cerebrospinal-fluid barrier (BCSFB) (Landers and Richard 2017; Richardson et al. 2015). Both barriers are known to synthesize endogenous TTR. After excretion into the maternal blood circulation (i.e., apical side), placental TTR binds T_4 upon which the TTR-T_4 complex passes the placenta and is thought to be finally delivered at the fetal capillaries (Landers and Richard 2017). TTR produced by the choroid plexus epithelial cells is not excreted to the blood-facing (basolateral) side but, rather, binds intracellularly to the T_4 taken up by the cells and is then excreted into the cerebrospinal fluid, where it is distributed to the brain (Richardson et al. 2015). This transcellular route across the BCSFB seems especially relevant for TH transport to the developing brain (Johansson et al. 2008). The possible effect of TTR-binding xenobiotic compounds on the transport of TH across these barriers is a subject for further studies. In our opinion, such studies should also include the transport of the TTR-binding xenobiotics across these barriers.

Despite TTR's role in the delivery of TH at the target tissue, and the transport of TH across the barriers, an association between maternal TTR malfunctioning and neurodevelopmental disorders in children and infants has not been reported. TTR mutations in humans have been associated with peripheral neuropathy due to amyloid deposition (João and Saraiva 1995) but not to effects on the developing brain due to TH deficiency. On the other hand, no humans lacking TTR have been reported either. This suggests that TTR's role in transporting sufficient TH to the developing fetal brain is crucial for survival. This hypothesis, however, was

questioned when Episkopou et al. (1993) demonstrated that TTR-null mice were viable, fertile, and without an overt TH-deficient phenotype. Apparently, the absence of TTR-mediated TH transport to the developing fetal brain was compensated by transmembrane transporter proteins such as monocarboxylate transporters (e.g., Mct8) and organic anion transporting polypeptides (e.g., Oatp1c1). More recent studies, however, did report differences in brain development between TTR-null and wild-type mice, that is, a decrease in TH-dependent apoptosis of neural stem cells in the subventricular zone (Richardson et al. 2007) and a delay in TH-regulated events in central nervous system maturation (Monk et al. 2013). It is not known whether such effects also occur in humans and whether they affect cognition in children and infants.

The predictive value of the estimated 1.3–1.5% inhibition of T_4-binding to TTR in human blood by house dust contaminants at median concentration levels needs to be further put in perspective. So far, inhibitor binding to other proteins than TTR is not considered simply because no K_i values for other proteins are available. Inhibitor binding to other proteins may decrease the concentration of free inhibitor and thereby its bioavailability to compete with T_4 for TTR binding. On the other hand, the inhibitors may also bind to TBG and ALB and thereby compete for their T_4-binding capacity. The consequence of such binding for T_4 binding in general and for T_4 delivery by TTR can only be estimated if K_i values become available for the TBG-inhibitor and ALB-inhibitor complexes.

Furthermore, many TTR-binding house dust contaminants are not represented in the mixtures studied in the present paper, because their presence in house dust or human blood is unknown or because their TTR-binding potency is unknown. As shown for the SRM2585 house dust sample, the 16 PFAS, PBDE, PCB and halogenated phenolic compounds for which concentrations were available only contributed 1.2% to the overall TTR-binding potency of the house dust extract. This finding clearly illustrates that house dust contains many more TTR-binding compounds than we currently know. Similarly, Kollitz et al. (2018) demonstrated that house dust extracts significantly antagonized activation of the TH receptor β (TRβ) by T_3. TRβ antagonistic activity was negatively associated with free T_4 levels in residents from the sampled houses and positively correlated with the presence of 12 brominated or organophosphorus flame retardants in the house dust. Because all 12 contaminants were inactive as TRβ antagonists on an individual basis, these results suggest either a synergistic mechanism or the presence of unknown TRβ antagonistic contaminants in house dust co-occurring with the 12 flame retardants. Previous nontargeted screening studies (Rager et al. 2016; Rostkowski et al. 2019) have confirmed that house dust contains thousands of chemicals of which the identity is unknown, let alone their TH disrupting capacity. Still, the different patterns in major contributors to the TTR-binding potencies in the mixtures reflecting known TTR-binding compounds in human blood and house dust indicate that dust is not the only route of human exposure to TTR-binding compounds. Most likely, exposure through food also contributes significantly to levels of TTR-binding compounds in human blood.

Moreover, the present study focused on mixtures reflecting median serum concentrations in Nordic countries. Especially for PBDEs, it is well known that serum levels are 4–18 times higher in North American than in European populations (Bramwell et al. 2016; Hites 2004; Huang et al. 2014). The contribution of the PBDEs and their metabolites to the TTR-binding potency of the reconstituted serum mixtures tested in the present study, however, was negligible (Figure 3). This finding did not change if concentrations of PBDEs and their metabolites were multiplied by a worst-case factor of 20. Given the fact that regional differences in serum concentrations are less obvious for the other compounds included in the present study, the results obtained for the Nordic mixtures are expected to be representative for other regions as well.

As discussed above, no clear relationship has been found between exposure to TTR-binding compounds and circulating T_4 levels in humans. This may be due to the relatively small predicted effect size at median exposure levels, that is, 1.3–1.5% inhibition of T_4-TTR binding (Table 2). Similarly, Audet-Delage et al. (2013) found that concentrations of TTR-binding compounds in Inuit women of childbearing age were not high enough to affect TTR-mediated TH transport. Although this study population was considered to have a relatively high dietary exposure to persistent organic pollutants including PCBs, PBDEs, PFASs, and pentachlorophenol, the reported plasma concentrations of TTR-binding compounds in the Inuit women were in the same range (i.e., PFOSs) or lower (i.e., OH-CBs and pentachlorophenol) than the median concentrations in Nordic countries used for reconstituting the median exposure level mixture in the present study. Given the between-day variation in their TTR (11.9%) and T_4-TTR (19.7%) measurements (Audet-Delage et al. 2013), it is to be expected that a predicted effect size in the same range or lower than in the present study (i.e., 1.3% inhibition in T_4-TTR binding in maternal blood; Table 2) could not be detected in the Inuit women. We expect, however, that the absolute decrease in T_4-TTR binding corresponding to a relative decrease of 1.3–1.5% may have more impact on circulating TH levels in humans with low T_4 levels than in humans with normal T_4 levels. As such, we hypothesize that the presence of TTR-binding house dust contaminants in blood may especially aggravate the poor TH status in mothers with or prone to developing hypothyroidism or hyperthyroxinemia during early pregnancy, which is associated with impaired neurodevelopment in their offspring (Fan and Wu 2016; Henrichs et al. 2013; Korevaar et al. 2016; Morreale de Escobar 2003).

In conclusion, the TTR-binding potency of reconstituted mixtures of house dust contaminants was well described according to the principle of concentration addition. Moreover, it followed Pareto's principle as >80% of the observed inhibition could be explained by <20% of the compounds present in the mixture. Based on the observed bioassay responses, the median concentrations of house dust contaminants reported in maternal and infant human serum in Nordic countries were estimated to cause a 1.3–1.5% inhibition in T_4-TTR binding in human blood. In the high-end concentration range, these estimates even reached 4.9–6.2% inhibition levels. This lack in margin of exposure toward TTR-inhibiting concentrations in blood is unfavorable given the role of TTR in delivery of TH to target tissues and its role in assisting TH to cross the placenta and the BCSFB. Possibly, the estimated inhibition levels may especially have impact on the developing fetal brain in cases of maternal hypothyroidism or hypothyroxinemia.

References

Alshehri B, D'Souza DG, Lee JY, Petratos S, Richardson SJ. 2015. The diversity of mechanisms influenced by transthyretin in neurobiology: development, disease

and endocrine disruption. J Neuroendocrinol 27(5):303–323, PMID: 25737004, https://doi.org/10.1111/jne.12271.

Altenburger R, Scholze M, Busch W, Escher BI, Jakobs G, Krauss M, et al. 2018. Mixture effects in samples of multiple contaminants—an inter-laboratory study with manifold bioassays. Environ Int 114:95–106, PMID: 29499452, https://doi.org/10.1016/j.envint.2018.02.013.

Athanasiadou M, Cuadra SN, Marsh G, Bergman Å, Jakobsson K. 2008. Polybrominated diphenyl ethers (PBDEs) and bioaccumulative hydroxylated PBDE metabolites in young humans from Managua, Nicaragua. Environ Health Perspect 116(3):400–408, PMID: 18335110, https://doi.org/10.1289/ehp.10713.

Audet-Delage Y, Ouellet N, Dallaire R, Dewailly E, Ayotte P. 2013. Persistent organic pollutants and transthyretin-bound thyroxin in plasma of Inuit women of childbearing age. Environ Sci Technol 47(22):13086–13092, PMID: 24160776, https://doi.org/10.1021/es4027634.

Bergman Å, Klasson-Wehler E, Kuroki H. 1994. Selective retention of hydroxylated PCB metabolites in blood. Environ Health Perspect 102(5):464–469, PMID: 8593850, https://doi.org/10.1289/ehp.94102464.

Besis A, Samara C. 2012. Polybrominated diphenyl ethers (PBDEs) in the indoor and outdoor environments—a review on occurrence and human exposure. Environ Pollut 169:217–229, PMID: 22578798, https://doi.org/10.1016/j.envpol.2012.04.009.

Bramwell L, Glinianaia SV, Rankin J, Rose M, Fernandes A, Harrad S, et al. 2016. Associations between human exposure to polybrominated diphenyl ether flame retardants via diet and indoor dust, and internal dose: a systematic review. Environ Int 92–93:680–694, PMID: 27066981, https://doi.org/10.1016/j.envint.2016.02.017.

Darnerud PO, Morse D, Klasson-Wehler E, Brouwer A. 1996. Binding of a 3,3′,4,4′-tetrachlorobiphenyl (CB-77) metabolite to fetal transthyretin and effects on fetal thyroid hormone levels in mice. Toxicology 106(1–3):105–114, PMID: 8571380, https://doi.org/10.1016/0300-483x(95)03169-g.

De Boer J, Ballesteros-Gómez A, Leslie HA, Brandsma SH, Leonards PEG. 2016. Flame retardants: dust—and not food—might be the risk. Chemosphere 150:461–464, PMID: 26765313, https://doi.org/10.1016/j.chemosphere.2015.12.124.

Denison MS, Nagy SR. 2003. Activation of the aryl hydrocarbon receptor by structurally diverse exogenous and endogenous chemicals. Annu Rev Pharmacol Toxicol 43:309–334, PMID: 12540743, https://doi.org/10.1146/annurev.pharmtox.43.100901.135828.

EFSA (European Food Safety Authority). 2005. Opinion of the Scientific Panel on contaminants in the food chain [CONTAM] related to the presence of non dioxin-like polychlorinated biphenyls (PCB) in feed and food. EFSA J 3(11):284, https://doi.org/10.2903/j.efsa.2005.284.

EFSA. 2011a. Scientific opinion on polybrominated diphenyl ethers (PBDEs) in food. EFSA J 9(5):2156, https://doi.org/10.2903/j.efsa.2011.2156.

EFSA. 2011b. Scientific opinion on tetrabromobisphenol A (TBBPA) and its derivatives in food. EFSA J 9(12):2477, https://doi.org/10.2903/j.efsa.2011.2477.

EFSA. 2018. Risk to human health related to the presence of perfluorooctane sulfonic acid and perfluorooctanoic acid in food. EFSA J 16(12):5194, https://doi.org/10.2903/j.efsa.2018.5194.

Episkopou V, Maeda S, Nishiguchi S, Shimada K, Gaitanaris GA, Gottesman ME, et al. 1993. Disruption of the transthyretin gene results in mice with depressed levels of plasma retinol and thyroid hormone. Proc Natl Acad Sci USA 90(6):2375–2379, PMID: 8384721, https://doi.org/10.1073/pnas.90.6.2375.

Fan X, Wu L. 2016. The impact of thyroid abnormalities during pregnancy on subsequent neuropsychological development of the offspring: a meta-analysis. J Matern Fetal Neonatal Med 29(24):3971–3976, PMID: 26988121, https://doi.org/10.3109/14767058.2016.1152248.

Faust M, Altenburger R, Backhaus T, Blanck H, Boedeker W, Gramatica P, et al. 2003. Joint algal toxicity of 16 dissimilarly acting chemicals is predictable by the concept of independent action. Aquat Toxicol 63(1):43–63, PMID: 12615420, https://doi.org/10.1016/s0166-445x(02)00133-9.

Feldt-Rasmussen U, Rasmussen ÅK. 2007. Thyroid hormone transport and utilization. In: *Diseases of the Thyroid in Childhood and Adolescence*, vol 3. Krassas GE, Rivkees SA, Kiess W, eds. Basel, Switzerland: Karger, 80–103.

Greco WR, Bravo G, Parsons JC. 1995. The search for synergy: a critical review from a response surface perspective. Pharmacol Rev 47(2):331–385, PMID: 7568331.

Gutleb AC, Cenijn P, van Velzen M, Lie E, Ropstad E, Skaare JU, et al. 2010. In vitro assay shows that PCB metabolites completely saturate thyroid hormone transport capacity in blood of wild polar bears (*Ursus maritimus*). Environ Sci Technol 44(8):3149–3154, PMID: 20345174, https://doi.org/10.1021/es903029j.

Hallgren S, Darnerud PO. 2002. Polybrominated diphenyl ethers (PBDEs), polychlorinated biphenyls (PCBs) and chlorinated paraffins (CPs) in rats—testing interactions and mechanisms for thyroid hormone effects. Toxicology 177(2–3):227–243, PMID: 12135626, https://doi.org/10.1016/s0300-483x(02)00222-6.

Hallinger DR, Murr AS, Buckalew AR, Simmons SO, Stoker TE, Laws SC. 2017. Development of a screening approach to detect thyroid disrupting chemicals that inhibit the human sodium iodide symporter (NIS). Toxicol In Vitro 40:66–78, PMID: 27979590, https://doi.org/10.1016/j.tiv.2016.12.006.

Hamers T, Kamstra JH, Sonneveld E, Murk AJ, Visser TJ, Van Velzen MJM, et al. 2008. Biotransformation of brominated flame retardants into potentially endocrine-disrupting metabolites, with special attention to 2,2′,4,4′-tetrabromodiphenyl ether (BDE-47). Mol Nutr Food Res 52(2):284–298, PMID: 18161906, https://doi.org/10.1002/mnfr.200700104.

Henrichs J, Ghassabian A, Peeters RP, Tiemeier H. 2013. Maternal hypothyroxinemia and effects on cognitive functioning in childhood: how and why? Clin Endocrinol (Oxf) 79(2):152–162, PMID: 23600900, https://doi.org/10.1111/cen.12227.

Hites RA. 2004. Polybrominated diphenyl ethers in the environment and in people: a meta-analysis of concentrations. Environ Sci Technol 38(4):945–956, PMID: 14998004, https://doi.org/10.1021/es035082g.

Huang F, Wen S, Li J, Zhong Y, Zhao Y, Wu Y. 2014. The human body burden of polybrominated diphenyl ethers and their relationships with thyroid hormones in the general population in Northern China. Sci Total Environ 466–467:609–615, PMID: 23959216, https://doi.org/10.1016/j.scitotenv.2013.07.008.

Jahnke GD, Choksi NY, Moore JA, Shelby MD. 2004. Thyroid toxicants: assessing reproductive health effects. Environ Health Perspect 112(3):363–368, PMID: 14998754, https://doi.org/10.1289/ehp.6637.

João M, Saraiva MJ. 1995. Transthyretin mutations in wealth and disease. Hum Mutat 5(3):191–196, PMID: 7599630, https://doi.org/10.1002/humu.1380050302.

Johansson PA, Dziegielewska KM, Liddelow SA, Saunders NR. 2008. The blood-CSF barrier explained: when development is not immaturity. Bioessays 30(3):237–248, PMID: 18293362, https://doi.org/10.1002/bies.20718.

Kato S, Itoh S, Yuasa M, Baba T, Miyashita C, Sasaki S, et al. 2016. Association of perfluorinated chemical exposure in utero with maternal and infant thyroid hormone levels in the Sapporo cohort of Hokkaido Study on the Environment and Children's Health. Environ Health Prev Med 21(5):334–344, PMID: 27137816, https://doi.org/10.1007/s12199-016-0534-2.

Kim DH, Kim UJ, Kim HY, Choi SD, Oh JE. 2016. Perfluoroalkyl substances in serum from South Korean infants with congenital hypothyroidism and healthy infants—its relationship with thyroid hormones. Environ Res 147:399–404, PMID: 26950028, https://doi.org/10.1016/j.envres.2016.02.037.

Kim SK, Kim KS, Sang HH. 2016. Overview on relative importance of house dust ingestion in human exposure to polybrominated diphenyl ethers (PBDEs): international comparison and Korea as a case. Sci Total Environ 571:82–91, PMID: 27471979, https://doi.org/10.1016/j.scitotenv.2016.07.068.

Klopčič I, Skledar DG, Mašič LP, Dolenc MS. 2016. Comparison of *in vitro* hormone activities of novel flame retardants TBB, TBPH and their metabolites TBBA and TBMEPH using reporter gene assays. Chemosphere 160:244–251, PMID: 27380226, https://doi.org/10.1016/j.chemosphere.2016.06.091.

Kollitz EM, Kassotis CD, Hoffman K, Ferguson PL, Sosa JA, Stapleton HM. 2018. Chemical mixtures isolated from house dust disrupt thyroid receptor β signaling. Environ Sci Technol 52(20):11857–11864, PMID: 30212187, https://doi.org/10.1021/acs.est.8b03283.

Korevaar TIM, Muetzel R, Medici M, Chaker L, Jaddoe VWV, de Rijke YB, et al. 2016. Association of maternal thyroid function during early pregnancy with offspring IQ and brain morphology in childhood: a population-based prospective cohort study. Lancet Diabetes Endocrinol 4(1):35–43, PMID: 26497402, https://doi.org/10.1016/S2213-8587(15)00327-7.

Kortenkamp A, Scholze M, Ermler S. 2014. Mind the gap: can we explain declining male reproductive health with known antiandrogens? Reproduction 147(4):515–527, PMID: 24435164, https://doi.org/10.1530/REP-13-0440.

Kretschmer XC, Baldwin WS. 2005. CAR and PXR: xenosensors of endocrine disrupters? Chem Biol Interact 155(3):111–128, PMID: 16054614, https://doi.org/10.1016/j.cbi.2005.06.003.

Landers K, Richard K. 2017. Traversing barriers—how thyroid hormones pass placental, blood-brain and blood-cerebrospinal fluid barriers. Mol Cell Endocrinol 458:22–28, PMID: 28153799, https://doi.org/10.1016/j.mce.2017.01.041.

Leusch FDL, Aneck-Hahn NH, Cavanagh J-A, Du Pasquier D, Hamers T, Hebert A, et al. 2018. Comparison of *in vitro* and *in vivo* bioassays to measure thyroid hormone disrupting activity in water extracts. Chemosphere 191:868–875, PMID: 29107228, https://doi.org/10.1016/j.chemosphere.2017.10.109.

Lewandowski TA, Seeley MR, Beck BD. 2004. Interspecies differences in susceptibility to perturbation of thyroid homeostasis: a case study with perchlorate. Regul Toxicol Pharmacol 39(3):348–362, PMID: 15135213, https://doi.org/10.1016/j.yrtph.2004.03.002.

Liu J, Liu Y, Barter R, Klaassen C. 1995. Alteration of thyroid homeostasis by UDP-glucuronosyltransferase inducers in rats: a dose-response study. J Pharmacol Exp Ther 273(2):977–985, PMID: 7752103.

Makey CM, McClean MD, Braverman LE, Pearce EN, He X, Sjödin A, et al. 2016. Polybrominated diphenyl ether exposure and thyroid function tests in North American adults. Environ Health Perspect 124(4):420–425, PMID: 26372669, https://doi.org/10.1289/ehp.1509755.

Manzano-Salgado CB, Casas M, Lopez-Espinosa MJ, Ballester F, Basterrechea M, Grimalt JO, et al. 2015. Transfer of perfluoroalkyl substances from mother to fetus in a Spanish birth cohort. Environ Res 142:471–478, PMID: 26257032, https://doi.org/10.1016/j.envres.2015.07.020.

Meerts I, Assink Y, Cenijn PH, Van Den Berg JHJ, Weijers BM, Bergman Å, et al. 2002. Placental transfer of a hydroxylated polychlorinated biphenyl and effects on fetal and maternal thyroid hormone homeostasis in the rat. Toxicol Sci 68(2):361–371, PMID: 12151632, https://doi.org/10.1093/toxsci/68.2.361.

Mendel CM. 1989. The free hormone hypothesis: a physiologically based mathematical model. Endocr Rev 10(3):232–274, PMID: 2673754, https://doi.org/10.1210/edrv-10-3-232.

Mendel CM, Cavalieri RR, Weisiger RA. 1988. Uptake of thyroxine by the perfused rat liver: implications for the free hormone hypothesis. Am J Physiol 255(2 Pt 1):E110–E119, PMID: 3407767, https://doi.org/10.1152/ajpendo.1988.255.2.E110.

Mercier F, Glorennec P, Thomas O, Le Bot B. 2011. Organic contamination of settled house dust, a review for exposure assessment purposes. Environ Sci Technol 45(16):6716–6727, PMID: 21667945, https://doi.org/10.1021/es200925h.

Monk JA, Sims NA, Dziegielewska KM, Weiss RE, Ramsay RG, Richardson SJ. 2013. Delayed development of specific thyroid hormone-regulated events in transthyretin null mice. Am J Physiol Endocrinol Metab 304(1):E23–E31, PMID: 23092911, https://doi.org/10.1152/ajpendo.00216.2012.

Morreale de Escobar G. 2003. Maternal hypothyroxinemia versus hypothyroidism and potential neurodevelopmental alterations of her offspring. Ann Endocrinol (Paris) 64(1):51–52, PMID: 12707634.

Neubig R. 2011. Fitting binding of fluorescent ligands. Knowledgebase Article #1725. https://www.graphpad.com/support/faq/fitting-binding-of-fluorescent-ligands/ [accessed 8 January 2020].

Nikolovska-Coleska Z, Wang R, Fang X, Pan H, Tomita Y, Li P, et al. 2004. Development and optimization of a binding assay for the XIAP BIR3 domain using fluorescence polarization. Anal Biochem 332(2):261–273, PMID: 15325294, https://doi.org/10.1016/j.ab.2004.05.055.

NIST (National Institute of Standards and Technology). 2018. Certificate of Analysis Standard Reference Material® 2585. Organic Contaminants in House Dust. https://www-s.nist.gov/srmors/certificates/2585.pdf [accessed 27 November 2019].

Olsen GW, Burris JM, Burlew MM, Mandel JH. 2003. Epidemiologic assessment of worker serum perfluorooctanesulfonate (PFOS) and perfluorooctanoate (PFOA) concentrations and medical surveillance examinations. J Occup Environ Med 45(3):260–270, PMID: 12661183, https://doi.org/10.1097/01.jom.0000052958.59271.10.

Ouyang X, Froment J, Leonards PEG, Christensen G, Tollefsen KE, de Boer J, et al. 2017. Miniaturization of a transthyretin binding assay using a fluorescent probe for high throughput screening of thyroid hormone disruption in environmental samples. Chemosphere 171:722–728, PMID: 28063299, https://doi.org/10.1016/j.chemosphere.2016.12.119.

Park J-S, Bergman Å, Linderholm L, Athanasiadou M, Kocan A, Petrik J, et al. 2008. Placental transfer of polychlorinated biphenyls, their hydroxylated metabolites and pentachlorophenol in pregnant women from eastern Slovakia. Chemosphere 70(9):1676–1684, PMID: 17764717, https://doi.org/10.1016/j.chemosphere.2007.07.049.

Paul KB, Hedge JM, Rotroff DM, Hornung MW, Crofton KM, Simmons SO. 2014. Development of a thyroperoxidase inhibition assay for high-throughput screening. Chem Res Toxicol 27(3):387–399, PMID: 24383450, https://doi.org/10.1021/tx400310w.

Pruckmayr G, Wu TK. 1978. Macrocyclic tetrahydrofuran oligomers. 2. Formation of macrocycles in the polymerization of tetrahydrofuran with triflic acid. Macromolecules 11(1):265–270, https://doi.org/10.1021/ma60061a049.

Purkey HE, Dorrell MI, Kelly JW. 2001. Evaluating the binding selectivity of transthyretin amyloid fibril inhibitors in blood plasma. Proc Natl Acad Sci USA 98(10):5566–5571, PMID: 11344299, https://doi.org/10.1073/pnas.091431798.

Rager JE, Strynar MJ, Liang S, McMahen RL, Richard AM, Grulke CM, et al. 2016. Linking high resolution mass spectrometry data with exposure and toxicity forecasts to advance high-throughput environmental monitoring. Environ Int 88:269–280, PMID: 26812473, https://doi.org/10.1016/j.envint.2015.12.008.

Ren XM, Guo LH. 2012. Assessment of the binding of hydroxylated polybrominated diphenyl ethers to thyroid hormone transport proteins using a site-specific fluorescence probe. Environ Sci Technol 46(8):4633–4640, PMID: 22482873, https://doi.org/10.1021/es2046074.

Richardson SJ. 2007. Cell and molecular biology of transthyretin and thyroid hormones. Int Rev Cytol 258:137–193, PMID: 17338921, https://doi.org/10.1016/S0074-7696(07)58003-4.

Richardson SJ, Lemkine GF, Alfama G, Hassani Z, Demeneix BA. 2007. Cell division and apoptosis in the adult neural stem cell niche are differentially affected in transthyretin null mice. Neurosci Lett 421(3):234–238, PMID: 17574756, https://doi.org/10.1016/j.neulet.2007.05.040.

Richardson SJ, Wijayagunaratne RC, D'Souza DG, Darras VM, Van Herck S. 2015. Transport of thyroid hormones via the choroid plexus into the brain: the roles of transthyretin and thyroid hormone transmembrane transporters. Front Neurosci 9:66, PMID: 25784853, https://doi.org/10.3389/fnins.2015.00066.

Robbins J. 2002. Transthyretin from discovery to now. Clin Chem Lab Med 40(12):1183–1190, PMID: 12553418, https://doi.org/10.1515/CCLM.2002.208.

Robbins J, Edelhoch H. 1986. Hormone transport in blood—thyroid hormone transport proteins: their nature, biosynthesis, and metabolism. In: Werner's the Thyroid. Ingbar SH, Braverman LE, eds. Philadelphia PA: J.B. Lippincott, 116–127.

Roos R, Andersson PL, Halldin K, Håkansson H, Westerholm E, Hamers T, et al. 2011. Hepatic effects of a highly purified 2,2′,3,4,4′,5,5′-heptachlorbiphenyl (PCB 180) in male and female rats. Toxicology 284(1–3):42–53, PMID: 21458519, https://doi.org/10.1016/j.tox.2011.03.013.

Rostkowski P, Haglund P, Aalizadeh R, Alygizakis N, Thomaidis N, Arandes JB, et al. 2019. The strength in numbers: comprehensive characterization of house dust using complementary mass spectrometric techniques. Anal Bioanal Chem 411(10):1957–1977, PMID: 30830245, https://doi.org/10.1007/s00216-019-01615-6.

Salvatore D, Davies TF, Schlumberger M-J, Hay ID, Larsen PR, 2016. Thyroid physiology and diagnostic evaluation of patients with thyroid disorders. In: Williams Textbook of Endocrinology. 13th ed. Melmed S, Polonsky KS, Larsen PR, Kronenberg HM, eds. Philadelphia, PA: Elsevier, 334–368.

Scholze M, Boedeker W, Faust M, Backhaus T, Altenburger R, Grimme LH. 2001. A general best-fit method for concentration-response curves and the estimation of low-effect concentrations. Environ Toxicol Chem 20(2):448–457, PMID: 11351447, https://doi.org/10.1002/etc.5620200228.

Scholze M, Silva E, Kortenkamp A. 2014. Extending the applicability of the dose addition model to the assessment of chemical mixtures of partial agonists by using a novel toxic unit extrapolation method. PLoS One 9(2):e88808, PMID: 24533151, https://doi.org/10.1371/journal.pone.0088808.

Schussler GC. 2000. The thyroxine-binding proteins. Thyroid 10(2):141–149, PMID: 10718550, https://doi.org/10.1089/thy.2000.10.141.

Shelby MK, Klaassen CD. 2006. Induction of rat UDP-glucuronosyltransferases in liver and duodenum by microsomal enzyme inducers that activate various transcriptional pathways. Drug Metab Dispos 34(10):1772–1778, PMID: 16855052, https://doi.org/10.1124/dmd.106.010397.

Shrestha S, Bloom MS, Yucel R, Seegal RF, Rej R, McCaffrey RJ, et al. 2017. Perfluoroalkyl substances, thyroid hormones, and neuropsychological status in older adults. Int J Hyg Environ Health 220(4):679–685, PMID: 28065522, https://doi.org/10.1016/j.ijheh.2016.12.013.

Stapleton HM, Eagle S, Anthopolos R, Wolkin A, Miranda ML. 2011. Associations between polybrominated diphenyl ether (PBDE) flame retardants, phenolic metabolites, and thyroid hormones during pregnancy. Environ Health Perspect 119(10):1454–1459, PMID: 21715241, https://doi.org/10.1289/ehp.1003235.

Taheri M, Haghpanah T, Meftahi GH, Esfahlani MA, Gloshan F, Esmailpour K, et al. 2018. Mild permanent chronic thyroid hormones insufficiency induces cognitive dysfunction in the adult male and female rats. J Appl Pharm Sci 8:100–106, https://doi.org/10.7324/JAPS.2018.8716.

Van den Eede N, Dirtu AC, Ali N, Neels H, Covaci A. 2012. Multi-residue method for the determination of brominated and organophosphate flame retardants in indoor dust. Talanta 89:292–300, PMID: 22284495, https://doi.org/10.1016/j.talanta.2011.12.031.

Vansell NR, Klaassen CD. 2002. Increase in rat liver UDP-glucuronosyltransferase mRNA by microsomal enzyme inducers that enhance thyroid hormone glucuronidation. Drug Metab Dispos 30(3):240–246, PMID: 11854140, https://doi.org/10.1124/dmd.30.3.240.

Vranckx R, Savu L, Maya M, Nunez EA. 1990. Characterization of a major development-regulated serum thyroxine-binding globulin in the euthyroid mouse. Biochem J 271(2):373–379, PMID: 1700701, https://doi.org/10.1042/bj2710373.

Wang J, Hallinger DR, Murr AS, Buckalew AR, Simmons SO, Laws SC, et al. 2018. High-throughput screening and quantitative chemical ranking for sodium-iodide symporter inhibitors in ToxCast phase I chemical library. Environ Sci Technol 52(9):5417–5426, PMID: 29611697, https://doi.org/10.1021/acs.est.7b06145.

Weiss JM, Andersson PL, Lamoree MH, Leonards PEG, van Leeuwen SPJ, Hamers T. 2009. Competitive binding of poly- and perfluorinated compounds to the thyroid hormone transport protein transthyretin. Toxicol Sci 109(2):206–216, PMID: 19293372, https://doi.org/10.1093/toxsci/kfp055.

Weiss JM, Andersson PL, Zhang J, Simon E, Leonards PEG, Hamers T, et al. 2015. Tracing thyroid hormone-disrupting compounds: database compilation and structure-activity evaluation for an effect-directed analysis of sediment. Anal Bioanal Chem 407(19):5625–5634, PMID: 25986900, https://doi.org/10.1007/s00216-015-8736-9.

Zhang J, Kamstra JH, Ghorbanzadeh M, Weiss JM, Hamers T, Andersson PL. 2015. In silico approach to identify potential thyroid hormone disruptors among currently known dust contaminants and their metabolites. Environ Sci Technol 49(16):10099–10107, PMID: 26207645, https://doi.org/10.1021/acs.est.5b01742.

Zhang J, Li Y, Gupta AA, Nam K, Andersson PL. 2016. Identification and molecular interaction studies of thyroid hormone receptor disruptors among household dust contaminants. Chem Res Toxicol 29(8):1345–1354, PMID: 27410513, https://doi.org/10.1021/acs.chemrestox.6b00171.

Zhao X, Wang H, Li J, Shan Z, Teng W, Teng X. 2015. The correlation between poly-brominated diphenyl ethers (PBDEs) and thyroid hormones in the general population: a meta-analysis. PLoS One 10(5):e0126989, PMID: 25992849, https://doi.org/10.1371/journal.pone.0126989.

Zheng M-Y, Li X-H, Zhang Y, Yang Y-L, Wang W-Y, Tian Y. 2017. Partitioning of polybrominated biphenyl ethers from mother to fetus and potential health-related implications. Chemosphere 170:207–215, PMID: 28006755, https://doi.org/10.1016/j.chemosphere.2016.11.136.

Zota AR, Park JS, Wang Y, Petreas M, Zoeller RT, Woodruff TJ. 2011. Polybrominated diphenyl ethers, hydroxylated polybrominated diphenyl ethers, and measures of thyroid function in second trimester pregnant women in California. Environ Sci Technol 45(18):7896–7905, PMID: 21830753, https://doi.org/10.1021/es200422b.